BIOSENSORS FOR ENVIRONMENTAL MONITORING VIA BIOINHIBITION

by

Tao Wang

A dissertation submitted to the faculty of
The University of Utah
in partial fulfillment of the requirements for the degree of

Doctor of Philosophy

Department of Chemistry

The University of Utah

August 2017

The University of Utah Graduate School

STATEMENT OF DISSERTATION APPROVAL

The dissertation of **Tao Wang**

has been approved by the following supervisory committee members:

Shelley D. Minteer	, Chair	**3/30/2017** Date Approved
Henry S. White	, Member	**4/11/2017** Date Approved
Marc D. Porter	, Member	**4/4/2017** Date Approved
Michael D. Morse	, Member	**4/5/2017** Date Approved
Bruce K. Gale	, Member	**4/10/2017** Date Approved

and by **Cynthia J. Burrows**, Chair/Dean of

the Department/College/School of **Chemistry**

and by David B. Kieda, Dean of The Graduate School.

ABSTRACT

Biosensors are devices that recognize, analyze, and transduce signal for detection via biological materials with bio-recognition properties. As of now, almost all kinds of biomaterials, including microbial cells, organelles, proteins, and nucleic acid, have been used for biosensors. In this dissertation, two kinds of biomaterials, enzymes and organelles, have been used for novel biosensor development. The primary focus of the research is the inhibition mechanism of laccase and mitochondria by different environmental toxins, like arsenic and pesticides.

In Chapter 2, a laccase-based biosensor was developed for arsenic sensing. Inhibition of oxygen reduction by arsenic was observed electrochemically via laccase immobilized with anthracene-modified multiwalled carbon nanotubes on a Toray carbon paper electrode. First, it was found that laccase is inhibited by arsenite and arsenate, and the inhibition mechanism was further determined as mixed inhibition (with preference to an uncompetitive inhibition model). Second, the laccase-modified electrodes were then fabricated into a self-powered biosensor with flavin-adenine-dinucleotide-dependent glucose dehydrogenase-based bioanodes. The biosensor was operated at 10% of its maximum current and demonstrated a detection limit of 13 µM for arsenite and 132 µM for arsenate.

In Chapter 3, a mitochondrial paper-based biosensor was fabricated.

Coupled mitochondria were isolated from bovine heart and demonstrated an amperometrical detection limit of 20 nM for malathion, a common pesticide. The inhibition mechanism by malathion to mitochondrial metabolism was studied electrochemically and was determined to be uncoupling rather than inhibition.

In Chapter 4, the inhibition mechanism of mitochondria by rotenone, carboxin, and antimycin was studied. It was also discovered that the synergy between riboflavin derivatives and ubiquinone can be altered by using different solvents during the electrode fabrication process. A further study indicated that lipid membrane is capable of altering the reaction dominance between ubiquinone and riboflavin derivatives. Finally, it was discovered that mitochondria release riboflavin derivatives under inhibition and it is believed that this alteration of the micro-environment was the cause of the change in mitochondrial electrochemistry when mitochondria were inhibited.

TABLE OF CONTENTS

LIST OF FIGURES

ACKNOWLEGEMENTS

Special thanks to my advisor, Dr. Minteer, who set a gold standard in academia and will always be inspiring to me for the rest of my career. I'm also grateful to many fellow graduate students and postdoctoral researchers in Minteer's group, whose warm and sincere support, both scientifically and morally, helped me greatly to work through graduate school. Special thanks go to Dr. Ross Milton, Dr. Sofiene Abdellaoui, and Dr. Kamrul Hasan, who offered great help on enzymatic electrochemistry and biofuel cells. I am also thankful to the USDA for funding support.

CHAPTER 1

INTRODUCTION

1.1. Overview of biosensor

A biosensor is a device that utilizes biological material for the quantitative detection of a specific analyte. The components of a biosensor usually include a biorecognition component and a transducing component.[1] Nowadays, biosensors utilize a very broad choice of materials for both components. For both the biorecognition component and the transducer, almost all of the available biomaterials, such as microbial cells, organelles, proteins, and nucleic acid, have been investigated. After only 60 years of development, both spectroscopic [2-7] and electrochemical biosensors[8-12] have been extensively researched and reported. A schematic of the biosensing process is shown in Figure 1.1.

The first biosensor was constructed back in the 1960s,[1,13] which was aimed at detecting glucose. The development of first-generation biosensors began by utilizing glucose oxidase to oxidize glucose and detect the H_2O_2 generated by the enzyme as a coupled side reaction. In this application, glucose oxidase oxidizes glucose to gluconolactone and reduces oxygen to H_2O_2. The concentration of glucose is analyzed by oxidizing the H_2O_2 generated by glucose oxidase with an electrode and correlating it with the glucose concentration. This type of biosensor

is still being extensively studied for the broad involvement of H_2O_2 in biological systems, since H_2O_2 is the product of O_2 reduction by many different kinds of enzyme in biological systems, and is therefore used for detection of glucose,[14-16] lactate,[17-19] lactose,[20-21] etc. However, these first-generation biosensors face a few technical problems such as dependency on oxygen and poor selectivity. Because of the oxygen dependence and the low solubility of oxygen in aqueous solutions, the sensitivity of these biosensors is limited. Additionally, many other common biological species, such as uric acid and acetaminophen,[22] are electrochemically active at the oxidation potential of H_2O_2, which limits selectivity. In order to overcome these problems, especially to increase the specificity of the biosensor and eliminate oxygen dependence, the second generation of biosensors were developed.

The second-generation biosensors utilize artificial mediators as electron acceptors instead of oxygen. These redox mediators are mostly organometallic redox active species that are reduced by the enzyme when the substrate is oxidized, or vice versa. The benefit of utilizing redox mediators is that the solubility of redox mediators is usually significantly greater than O_2, thus removing the kinetic limit caused by the concentration of O_2 and obtaining a much higher signal from the biosensors. Meanwhile, the large number of different redox mediators allows a broad choice of operating potential of biosensors, therefore avoiding the interference that H_2O_2 detection often encounters in a biological system. The choice of redox mediator is abundant for biosensors. A few commonly used redox mediators include ferrocene,[23-25] methylene blue,[26-28] and neutral red.[29-31] Initially,

mediators utilized for second-generation biosensors were solution-based, which made their fabrication process easy but limited the application potential of these biosensors severely due to the significant amount of mediator required, as well as limited current caused by transport limitations and degradation of mediator. Therefore, attempts to immobilize mediators at the electrode surface have also been performed. The most commonly used immobilization methods for redox mediators are tethering redox active molecules into a polymer backbone[32-34] or using pyrene π-π stacking systems.[35-38]

The third generation of biosensors, in the perspective of electrochemical biosensors, uses direct electron transfer (DET). One example of direct electron transfer is oxygen reduction of laccase where an anthracene-modified carbon nanotube is used to dock the T1 copper center towards the electrode and utilize the small distance (0.65 nm) for the electrons to tunnel between the enzyme and carbon.[39] However, for microbial cells, DET is more controversial since most of the DET reported for microbial cells involve electron transfer with an electrochemically active species produced by the microbial cells.

1.2. Electrochemical biosensor

Cost efficiency is the key factor to make electrochemical biosensors stand out in terms of market potential. Applications of electrochemical biosensors include implantable medical devices, field-deployable water monitoring devices, food quality monitoring, etc. The first biosensor utilized glucose oxidase,[1] an enzyme for glucose monitoring. During the developing process, a variety of biomaterials

were studied. Microbial materials were introduced to overcome a few drawbacks of using enzymes, such as short lifespans, long and costly purification processes, and the need to provide cofactors/coenzymes for the generation of measurable product, etc.[40] In most cases, microbial cells contain a large variety of enzymes that allows detection of a broad range of analytes, and they can be directly applied on the electrode without purification. However, the membrane structure of microbial cells limits the response time of microbial biosensors. To overcome that, organelle biosensors come into play. The goal for organelle biosensors is to merge the advantages of enzymatic and microbial biosensors to obtain a fast response while maintaining a relatively easy purification process. The diversity of biosensor materials has increased dramatically recently and novel materials such as DNA and tissue have been studied as well. While these novel materials are seen more and more commonly in recent publications, the primary categories of biosensor materials can be classified as enzymatic, microbial, organelle, and nucleic acid.

1.2.1 Enzymatic biosensors

Enzymes are a type of protein that catalyzes a specific category of chemical reactions. Enzymatic biosensors are by far the most studied biosensor and have the most widely used application. Enzymatic biosensors possess advantages such as outstanding specificity, rapid sensor response, and easy fabrication. Enzymatic biosensors can be classified into two categories: utilizing the analyte as the substrate, and using enzyme inhibition to detect an inhibitor. Now a vast variety of enzyme have been utilized as enzymatic biosensors with a wide choice of

substrates (such as glucose,[41-43] pyruvate,[44-46] lactate,[47-49] etc.), which allows enzymatic biosensors to be utilized in many fields like health care, food industry, and environmental monitoring.

1.2.1.1 Enzyme kinetics

The majority of enzymatic reactions can be described with the Michaelis-Menten enzyme kinetics model. In this case, the enzyme binds the substrate to form a complex and then the product is released whereas the enzyme is returned to its original form. This model can be divided into two specific stages: when the concentration of substrate is low, the reaction rate is linearly correlated to the concentration of substrate, whereas at high substrate concentration, the substrate saturates the enzyme and the reaction rate does not increase as the concentration of substrate increases. Two constants, K_M and V_{max}, are usually used to characterize an enzymatic catalysis system. K_M, the Michaelis constant, is the substrate concentration at half-maximum reaction rate, where V_{max} is the maximum reaction rate. The equation of the Michaelis-Menten enzyme kinetics model is shown as Equation 1.1.

$$v = \frac{V_{max}[S]}{K_M + [S]} \quad [1.1]$$

However, a significant amount of enzymes utilize more than one substrate and the turnover of those two substrate by the same enzyme is related. For instance, succinate dehydrogenase oxidizes succinate while it reduces ubiquonone. In this case, because of the dependency of those two reactions, the kinetics of succinate dehydrogenase cannot be described using the Michaelis-

Menten kinetics model. In this case, a double-placement mechanism is used to describe such a mechanism. The double-placement mechanism is more commonly characterized figuratively, most commonly with the Lineweaver-Burk plot, which will be described in the following section.

1.2.1.2 Lineweaver-Burk plot

The Lineweaver-Burk plot is commonly used to characterize a double-placement enzyme kinetics; it is also used to distinguish different enzyme inhibition types. The equation of the Lineweaver-Burk plot is derived from rearranging the Michaelis-Menten model shown as Equation 1.2.

$$\frac{1}{V} = \frac{K_M}{V_{max}}\frac{1}{[S]} + \frac{1}{V_{max}} \quad [1.2]$$

The Lineweaver-Burk plot can be used to distinguish different double-placement enzymatic reactions and enzyme inhibition. The double-placement enzyme reaction can be put into two categories depending on whether a ternary complex is formed during the reaction process or not. For double-placement reaction involving formation of a ternary complex, the enzyme binds both the substrates before releasing any product, whereas the binding of two substrate may or may not occur in a specific order. In the Lineweaver-Burk plot of a double-placement enzymatic reaction, when 1/V is plotted against 1/[S_1] under different [S_2], the Lineweaver-Burk plot is a series of intersecting lines.

Another case of double-placement enzymatic reaction is the Ping-Pong reaction, where the two reactions were sequential. In the Ping-Pong reaction, the turnover of the two substrates is dependent on each other. Specifically, the

enzyme turns over one of the substrates to one of the products while itself turning into an intermediate configuration; the intermediate enzyme then turns over the other substrate and returns to its original form. In the Lineweaver-Burk plot of a Ping-Pong reaction, when 1/V is plotted against $1/[S_1]$ under different $[S_2]$, the Lineweaver-Burk plot is a series of parallel lines.

Other than the Lineweaver-Burk plot, many other graphic tools have been used for analyzing enzyme kinetics. Aside from the most commonly used Lineweaver-Burk plot, there is the Eadie–Hofstee plot and Hanes–Woolf plot. The equations of the Eadie-Hofstee plot and Hanes-Woolf plot are shown individually in Equation 1.3 and 1.4.

$$v = V_{max} - K_M \frac{v}{[S]} \quad [1.3]$$

$$\frac{[S]}{v} = \frac{[S]}{V_{max}} + \frac{K_M}{V_{max}} \quad [1.4]$$

Comparing to the Linewear-Burk plot, in the Eadie-Hofstee plot, V_{max} is determined by the intersect and K_M is determined by the slope. The Hanes-Woolf plot is the most complicated in terms of determining kinetics parameters, where V_{max} can be determined from the slope of the plot and K_M/V_{max} can be determined from the intersect. Among all those graphic methods of determining kinetics parameters, the Linewear-Burk plot represents the most convenient method and thus is most commonly used.

1.2.1.3 Enzyme inhibition

The inhibition of enzymes can be classified into 2 categories, reversible inhibition and irreversible inhibition. In the case of reversible inhibition, the inhibitor

either binds to the enzyme or the enzyme substrate complex without causing destruction of the enzyme. In the case of irreversible inhibition, the binding of inhibitor and enzyme dysfunction the enzyme. A model to resolve the type of inhibition can be developed by analyzing the inhibition kinetics of a specific enzyme.

Most commonly, enzyme kinetics fit the Michaelis-Menten kinetics model. In this case, the enzyme binds the substrate to form a complex and then the product is released while the enzyme is returned to its original form. This model can be divided into two specific stages: when the concentration of the substrate is low, the reaction rate is linearly correlated to the concentration of the substrate, while at high substrate concentration, the substrate saturates the enzyme and the reaction rate does not increase as the concentration of the substrate increases. Two constants, K_M and V_{max}, are usually used to characterize an enzymatic catalysis system. K_M, the Michaelis constant, is the substrate concentration at half-maximum reaction rate, where V_{max} is the maximum reaction rate.

Reversible inhibition can be further classified into 3 sub-categories, competitive inhibition, uncompetitive inhibition, and noncompetitive inhibition. For competitive inhibition, the inhibitor directly binds to the active site of the enzyme; therefore, it acts as a competitor to the substrate. An indication of competitive inhibition is that K_M decreases while V_{max} stays the same. The Lineweaver-Burk plot of competitive inhibition under different concentration of inhibitors is a series of lines that converge on the y-axis. Uncompetitive inhibition happens when the inhibitor only binds to the enzyme-substrate complex. In this case, both K_M and V_{max} decreases. The Lineweaver-Burk plot of uncompetitive inhibition under

different concentration of inhibitors is a series of parallel lines. In the case of noncompetitive inhibition, the inhibitor binds to a non-active site of the enzyme and changes the enzyme configuration, rendering the enzyme incapable of binding the substrate. V_{max} decreases while K_M stays the same in the presence of a non-competitive inhibitor. The Lineweaver-Burk plot of noncompetitive inhibition under different concentration of inhibitors is a series of lines that converge on the x-axis. The last type of reversible enzyme inhibition is mixed inhibition, in which a combination of any of the above types of inhibition occur together, and the Lineweaver-Burk plot of mixed inhibition usually intersects but not on any of the axes.

1.2.1.4 Enzyme immobilization techniques

In the earliest era of biosensors, enzymes were utilized in solubilized form.[50-52] While solubilized enzyme is still used occasionally, this method of enzyme utilization is resource-demanding and the performance is subpar. To solve this problem, enzyme immobilization techniques were introduced. Immobilization of enzyme increases the surface concentration of enzyme on the transducer, as well as maintaining the biological activity of enzyme. The immobilization methods used in enzymatic biosensors include physical adsorption, covalent bonding, entrapping, and crosslinking.[53]

Physical adsorption is the easiest and most direct method of enzyme immobilization. Enzymes can adsorb on surfaces via Van Der Waal's forces or electrostatic interactions. This method applies to many different enzymes and is

still being used today. Some of the enzymes that can be fabricated into a biosensor by this method include urease, glucose oxidase, and horseradish peroxidase.[54-56]

Enzyme entrapment usually involves immobilizing enzymes within a three-dimensional (3-D) network. Many methods and materials have been reported for enzyme entrapment. Electropolymerization of compounds such as polyaniline and polypyrrole has been extensively used with enzymes like glucose oxidase,[57-58] horseradish peroxidase,[59] and uricase.[60-61] These conductive polymers offer a network for 3-D electron transfer between the enzymes and the electrode. Moreover, they allow a much better spatial utilization of enzymes, thus significantly increasing sensor response. In some other cases, a sol-gel network is commonly utilized. This category of enzyme entrapment exhibits great abundancy in terms of material choices. Sol-gel immobilization techniques use materials like silane derivatives, polysaccharide, etc. Among these materials, polysaccharide derivatives have shown good biocompatibility. It has been reported that enzymes entrapped in agarose (a polysaccharide derivative) can maintain activity for months.[62-63] Carbon paste and clay are also commonly used materials for enzyme entrapping. The performance of carbon paste can be manipulated by utilizing different binders, or by surface modification of the carbon.[64-65] As for clay, its inorganic matrix provides abundant surface area for entrapping enzymes. Many different enzymatic biosensors have been reported utilizing clay as an immobilization material for analytes such as glucose,[66] H_2O_2,[67] and urea.[68]

Crosslinking is defined as linking the enzyme to a surface with a crosslinking chemical, which covalently binds protein to surfaces.[69-71] In other cases where a

redox mediator is needed, crosslinking of the redox active polymer is involved. The crosslinking of such polymers creates a network that entraps the enzymes. The backbone of the polymer network expands the surface area of the electrode and allows charge to pass along the backbone by rapid self-exchange so higher current density can be obtained.

1.2.1.5 Applications of enzymatic biosensors

Applications of biosensors have always been the primary focus of this type of research. Glucose biosensors were the first kind of biosensor put into application and now possess a market of more than $2 billion.[72] In the concept of an artificial pancreas, biosensors for blood sugar monitoring are linked to an insulin pump as an automatic way to inject insulin when high blood sugar level is detected.[73] However, commercial applications of biosensors are rarely seen for other types of biosensor other than glucose biosensors.

Another potential field of application for enzymatic biosensors is environmental monitoring, where enzymatic biosensors show comparable response to traditional detecting methods. However, commercial applications in the category are rarely seen for biosensors, because they often lack specificity due to the difficulty of separating and distinguishing different toxins. However, the application of enzymatic biosensors in environmental science and engineering is still promising for the cost efficiency of enzymatic biosensors.

1.2.1.6 Laccase-based biosensors

Self-powered biosensors are among the most promising applications for biosensors and they are mostly constructed as enzymatic fuel cells. For enzymatic fuel cells, the enzyme options for enzymatic anodes are abundant, including glucose oxidase, glucose dehydrogenase, alcohol dehydrogenase, etc. However, the choices for biocathodes are limited. At present, the only enzymatic biocathodes reported extensively employ laccase or bilirubin oxidase. Compared to bilirubin oxidase, laccase is reported to be more sensitive to many different ions and inhibitors, such as azide, Cl^-, and F^-, making it a feasible biosensor material.

Laccase contains 3 copper centers: the T1 copper center is responsible for oxidizing phenol derivatives, while the T2 and T3 copper centers form a trinuclear (TNC) center which is responsible for reducing oxygen to water. Since laccase utilizes electrochemical active phenonl derivatives, such as 4-methoxybenzyl alcohol, 2,2'-azino-bis(3-ethylbenzothiazoline-6-sulphonic acid) and phenothiazine, as substrates, mediated electron transfer for laccase is feasible.[74] However, the T1 copper center of laccase is only 0.65 nm from the outside of laccase, which also makes it possible for laccase to perform direct electron transfer.[75] Direct electron transfer, in comparison to mediated electron transfer, does not undergo a potential loss between the enzyme and mediator and, therefore, theoretically provides higher energy output.

Although laccase itself possesses the capability of directly electron transfer, it does require a specific spatial arrangement between the enzyme and electrode to allow the shortest distance for the electrons to tunnel. Therefore, to improve the

electron transport efficiency, different docking techniques have been developed. Among these techniques, the most successful ones involve immobilizing anthracene on carbon nanotubes with either π-π stacking via pyrene[76] or by covalently binding anthracene directly on carbon nanotubes.[77]

Laccase has been studied as a biorecognition material for phenol compounds as part of wine analysis. Another application of laccase as a biosensor is oxygen sensing. For both of these kinds of analysis, laccase utilizes the analyte as substrate. As described before, laccase is also sensitive to different inhibitor analytes. The inhibition of laccase by different inhibitors can be put into a few different categories: the inhibition of laccase by F^- is irreversible inhibition, while laccase inhibition by Cl^- can be classified as competitive inhibition, and inhibition by H_2O_2 can be classified as noncompetitive inhibition.[39] Given the sensitivity of laccase to inhibitors, it has potential as an inhibition-based biosensor. For example, H_2O_2 could be identified by the fact that laccase regains activity with the addition of catalase.

1.2.2 Microbial biosensors

Compared to enzymatic biosensors, microbial biosensors possess advantages like better stability and good biomaterial accessibility. Just like enzymatic biosensors, microbial biosensors have an abundant choice of sensing motifs, such as *Pseudomonas putida,*[78] *E coli*,[79] and *Acidithiobacillus ferrooxidans*.[80] Various analytes have been reported for microbial biosensors; however, unlike enzymatic biosensors, the application of microbial biosensors in

the health care field is rare, mostly due to possible risk of infection.

1.2.2.1 Microbial cell immobilization

In terms of immobilization techniques, microbial cells offer more options than enzymes. Techniques used for enzyme immobilization, such as entrapment and absorption, can also be applied to microbial cells. However, unlike enzymes, which are single proteins, microbial cells contain a series of proteins for their biofunctionality and they are capable of growing and forming biofilms on different surfaces; therefore, they have the capability of attaching themselves on the transducer surface when proper stimuli is applied.

Biofilms are observed for multiple microbial species, such as *Geobacter* and *Shewanella*. In many cases, the formation of a biofilm is observed under specific stimuli - usually an electric potential. The term “biofilm” is more of a general concept and it includes different types of microbial cell “self-immobilization.” The exact mechanism of electron transfer in biofilms is complicated and differs between each individual microbial species. Conductive pili have been suggested by some researchers to be part of the mechanism of biofilm electrochemistry for species such as *Shewanella*, while other researchers claim that cytochromes and riboflavins are to be the responsible electrochemically active species for the same species under different immobilizing conditions.[81] It is hypothesized that the electrochemical mechanism of a biofilm is altered by the nature of the electrode surface; for example, carbon is selective to riboflavins whereas ITO is selective to cytochrome c. However, the mechanism is still under debate and a systematic

conclusion has not been drawn yet.

1.2.2.2 Applications of microbial biosensors

Abundant research has been performed for microbial biosensors. The analysis of organophosphate chemicals by microbial biosensors has been extensively studied.[1] For many microbial biosensors, the detection of organophosphate compounds relies on surface active proteins, such as organophosphorus hydrolase.[40] This protein has shown selectivity and sensitivity to many different organophosphate pesticides such as paraxon, parathion, and methyl parathion.[82-83] Another application of microbial biosensors is the measurement of Biochemical Oxygen Demand (BOD), a vital parameter in wastewater treatment. Instead of the traditional BOD measurement, which usually takes about a week, the process can be shortened by directly immobilizing microbes on the electrode. For instance, Kara *et al.* immobilized *P. Syringae* on an oxygen probe and obtained responses as fast as 3-5 min.[84]

Microbial biosensors have also shown potential for the detection of other environmental toxins. Phenols can be detected by *P. putida*[85] or *E. coli*.[86] Moreover, it is also reported that microbial biosensors can be used for detecting heavy metals, such as Cu^{2+} and Cr^{3+}.[80,87]

1.2.3 Organelle biosensors

Organelle biosensors primarily involve thylakoids and mitochondria. The idea of utilizing organelles for biosensors comes from combining the stability of a

microbial biosensor and the sensitivity and fast response time of enzymatic biosensors. The studies of electrochemically active species for organelle biosensors are similar to those for microbial biosensors. In studies involving organelles, cytochromes and quinones are the top pick for electrochemically active species.[88-91] Thylakoids have been studied for a pesticide biosensor and have shown competent sensitivity.[92] Mitochondria have also been tested as biosensors for pesticides[89] and nitroaromatic explosives, which are mitochondria uncouplers.[88] Mitochondria are also extensively studied in health-care-related topics for their vital role in apoptosis.[93-95]

1.3 Mitochondrial biosensors

Mitochondria are organelles that are responsible for the complete oxidation of pyruvate and synthesis of ATP. Mitochondria carry a complete set of Kreb's cycle enzymes for the complete oxidation of pyruvate. Mitochondria can also utilize fatty acids and amino acids as substrates. The complete oxidation of substrate in mitochondria usually starts with the transformation of the original substrate into acetyl-CoA; acetyl-CoA further enter the Krebs cycle for complete oxidation and the ATP synthesis is performed by the mitochondrial electron transport chain (ETC).

The electron transport chain is the key component in mitochondria for ATP synthesis. The electron transport chain contains NADH-ubiquinone oxidoreductase (complex I), acetyl-CoA-ubiquinone oxidoreductase (complex II), ubiquinone-cytochrome c oxidoreductase (complex III), and cytochrome c oxidase

(complex IV). Complex I and II are FAD containing proteins that pass electrons to ubiquinone, which is then oxidized by complex III. Complex III then reduces cytochrome c, a redox active protein residing between the mitochondrial inner and outer membranes, and the electron is finally passed to complex IV. Finally, complex IV reduces oxygen to water. The ATP synthase (complex V) is usually considered part of the electron transport chain, although no electron is passed to it from other complexes in the electron transport chain. A demonstration of the structure of mitochondrial electron transport chain is shown in Figure 1.2.

Mitochondria contain two membranes, an outer membrane and an inner membrane. In the process of total oxidation of pyruvate, fatty acids, and amino acids, complexes I, II, and IV pump protons from the mitochondrial matrix to the mitochondrial intermembrane space (the space between the mitochondrial outer and inner membranes), creating a proton gradient between the mitochondrial matrix and intermembrane space. The mitochondrial complex V utilizes the proton gradient generated by other complexes in the mitochondrial electron transport chain to synthesize ATP.

The fact that mitochondria contain multiple electrochemically active species, such as ubiquinone, cytochrome c, and cytochrome P450, makes it possible to make mitochondria into an electrochemical biosensor. The first electrochemistry of mitochondria, observed on a pyrolytic graphite electrode surface, was credited to cytochrome c and FAD/$FADH_2$.[96] Further study suggests that ubiquinone is more likely to be the electrochemically active species, as demonstrated by separately depleting ubiquinone or cytochrome c in mitochondria and comparing

the electrochemical behavior.[91] After the achievement of mitochondrial electrochemistry, mitochondria have been tested against different environmental toxins, such as parathion, paraquat, and malathion.[89,97] Mitochondria have also been shown to be sensitive to nitroaromatic compounds, a category of explosives that are also mitochondrial uncouplers, thus making them applicable to a self-powered biosensor for explosives sensing.[88]

1.3.1 Mitochondria uncoupling

As mentioned previously, mitochondrial complex V relies on the proton gradient between the mitochondrial matrix and intermembrane space to synthesize ATP. When mitochondria are healthy, the inner membrane itself is non-permeable to protons and the only way for protons to transport through the mitochondrial inner membrane is via complexes I, III, IV, and V. Proton outflow is regulated by complexes I, III, and IV, and proton inflow is regulated by complex V. When mitochondrial ETC are coupled (also described as when mitochondria are coupled), the activity of complex V is directly related to the activity of the rest of the mitochondrial ETC. However, when mitochondria are uncoupled due to either apoptosis, mitochondrial defect, or other illness, the permeability of the mitochondrial inner membrane is increased, the proton gradient is partially or totally lost, and thus the link between complex V's activity and the other ETC complexes is lost. This phenomenon is called mitochondria uncoupling.

The characterization of mitochondrial metabolism is performed by monitoring the oxygen consumption rate while inhibiting different components of

the mitochondrial electron transport chain or while uncoupling the whole mitochondria. A typical response under the inhibition of any part of the mitochondrial electron transport chain, even complex V, will be a decrease in the mitochondrial oxygen consumption rate, while the uncoupling of mitochondria will cause the mitochondrial oxygen consumption rate to reach its maximum value.

The mechanism of mitochondrial uncoupling is under extensive study and now, a commonly accepted theory is that mitochondrial uncoupling is performed by uncoupling proteins.[98] In healthy mitochondria, uncoupling proteins are responsible for regulating tissue temperature, as uncoupled respiration leads to heat production instead of ATP production. Another role of uncoupling proteins is to suppress the generation of reactive oxygen species,[98] which is why mitochondrial uncoupling is usually the first indication of mitochondrial apoptosis.

1.4 Overview of the dissertation

This research focuses on the mechanism and application of two different types of biosensors, a laccase-based biosensor for arsenic sensing (Chapter 2) and a mitochondrial biosensor for pesticide sensing and early diseases diagnosis (Chapters 3 and 4).

In Chapter 2, the inhibition of laccase by $As^{3+/5+}$ was first observed electrochemically via utilization of a laccase-modified electrode on anthracene-doped multiwall carbon nanotube-modified electrodes. The inhibition mechanism was determined by Lineweaver-Burk plot and Michaelis-Menten nonlinear regression and appeared to be mixed inhibition. The sensitivity was determined as

0.91 ± 0.07 mV/mM for arsenite and 0.98 ± 0.02 mV/mM for arsenate and the detection limit was determined as 13 µM for arsenite and 132 µM for arsenate.

In Chapter 3, the isolation of coupled mitochondria from bovine heart is reported. The coupled mitochondria were tested against one of the popular organophosphate pesticides, malathion, and were shown as an on-and-off biosensor with a detection limit of 20 nM. It was also determined that although malathion is reported as both a mitochondrial uncoupler and inhibitor, the mitochondrial toxicity of malathion observed via electrochemical methods is more prone to be classified as an uncoupler for mitochondria.

In Chapter 4, a novel mechanism was discovered for mitochondrial inhibition monitored electrochemically. Different inhibitors (rotenone and permethrin on complex I, carboxin on complex II, antimycin on complex III) were tested with mitochondria-modified electrodes and similar electrochemical responses were observed for all three inhibitors, which contradicts the previously accepted mechanism that the electrochemically active species in mitochondria is ubiquinone. Another category of electrochemically active species, riboflavin derivatives, were tested individually and in combination with ubiquinone. It was demonstrated that the effect of riboflavin derivatives on the observed ubiquinone electrochemical signal changed depending upon which solvent was used to modify electrodes. When aqueous casting solution was used, the presence of riboflavin derivatives induced a decrease in ubiquinone signal. When a nonaqueous casting solvent (ethanol) or lipid membrane was used, the ubiquinone signal was enhanced. This phenomenon, combined with the fact that mitochondria release

riboflavin species under inhibition, indicates that mitochondrial electrochemistry is caused by a combination of riboflavin derivatives and ubiquinone.

1.5 References

1 Guilbault, G. G.; Pravda, M.; Kreuzer, M.; O'Sullivan, C. *Anal. Lett.* **2004**, *37*, 1481.

2 Liedberg, B.; Nylander, C.; Lunström, I. *Sensors. Actuator.* **1983**, *4*, 299.

3 Homola, J. *Anal. Bioanal. Chem.* **2003**, *377*, 528.

4 Haes, A. J.; Van Duyne, R. P. *J. Am. Chem. Soc.* **2002**, *124*, 10596.

5 Shafer-Peltier, K. E.; Haynes, C. L.; Glucksberg, M. R.; Van Duyne, R. P. *J. Am. Chem. Soc.* **2003**, *125*, 588.

6 Notingher, I. *Sensors* **2007**, *7*, 1343.

7 Buckmaster, R.; Asphahani, F.; Thein, M.; Xu, J.; Zhang, M. *Analyst* **2009**, *134*, 1440.

8 Ducey, M. W.; Meyerhoff, M. E. *Electroanalysis* **1998**, *10*, 157.

9 Wang, J.; Cai, X.; Rivas, G.; Shiraishi, H.; Farias, P. A.; Dontha, N. *Anal. Chem.* **1996**, *68*, 2629.

10 Wang, J.; Rivas, G.; Fernandes, J. R.; Paz, J. L. L.; Jiang, M.; Waymire, R. *Anal. Chim. Acta* **1998**, *375*, 197.

11 Shervedani, R. K.; Mehrjardi, A. H.; Zamiri, N. *Bioelectrochemistry* **2006**, *69*, 201.

12 Unnikrishnan, B.; Palanisamy, S.; Chen, S.-M. *Biosens. Bioelectron.* **2013**, *39*, 70.

13 Chauhan, N.; Pundir, C. S. *Anal. Chim. Acta* **2011**, *701*, 66.

14 Carelli, D.; Centonze, D.; De Giglio, A.; Quinto, M.; Zambonin, P. G. *Anal. Chim. Acta* **2006**, *565*, 27.

15 Rodriguez, M.; Rivas, G. *Electroanalysis* **2001**, *13*, 1179.

16 Koopal, C.; Nolte, R. *Enzyme Microb. Technol.* **1994**, *16*, 402.

17 Dempsey, E.; Wang, J.; Smyth, M. R. *Talanta* **1993**, *40*, 445.

18 Yashina, E. I.; Borisova, A. V.; Karyakina, E. E.; Shchegolikhina, O. I.; Vagin, M. Y.; Sakharov, D. A.; Tonevitsky, A. G.; Karyakin, A. A. *Anal. Chem.* **2010**, *82*, 1601.

19 Marquette, C. A.; Blum, L. c. J. *Anal. Chim. Acta* **1999**, *381*, 1.

20 Liu, H.; Ying, T.; Sun, K.; Li, H.; Qi, D. *Anal. Chim. Acta* **1997**, *344*, 187.

21 Conzuelo, F.; Gamella, M.; Campuzano, S.; Ruiz, M.; Reviejo, A.; Pingarron, J. *J. Agric. Food. Chem.* **2010**, *58*, 7141.

22 Wang, J. *Electroanalysis* **2001**, *13*, 983.

23 Shim, N. Y.; Bernards, D. A.; Macaya, D. J.; DeFranco, J. A.; Nikolou, M.; Owens, R. M.; Malliaras, G. G. *Sensors* **2009**, *9*, 9896.

24 Li, J.; Xiao, L.-T.; Liu, X.-M.; Zeng, G.-M.; Huang, G.-H.; Shen, G.-L.; Yu, R.-Q. *Anal. Bioanal. Chem.* **2003**, *376*, 902.

25 Hodak, J.; Etchenique, R.; Calvo, E. J.; Singhal, K.; Bartlett, P. N. *Langmuir* **1997**, *13*, 2708.

26 Yao, H.; Li, N.; Xu, S.; Xu, J.-Z.; Zhu, J.-J.; Chen, H.-Y. *Biosens. Bioelectron.* **2005**, *21*, 372.

27 Ye, J.; Baldwin, R. P. *Anal. Chem.* **1988**, *60*, 2263.

28 Levin, R. L.; Degrange, M. A.; Bruno, G. F.; Del Mazo, C. D.; Taborda, D. J.; Griotti, J. J.; Boullon, F. J. *Ann. Thorac. Surg.* **2004**, *77*, 496.

29 Park, D. H.; Zeikus, J. G. *Appl. Environ. Microb.* **2000**, *66*, 1292.

30 Park, D. H.; Kim, S. K.; Shin, I. H.; Jeong, Y. J. *Biotechnol. Lett* **2000**, *22*, 1301.

31 Park, D.; Laivenieks, M.; Guettler, M.; Jain, M.; Zeikus, J. *Appl. Environ. Microb.* **1999**, *65*, 2912.

32 Albagli, D.; Bazan, G.; Schrock, R.; Wrighton, M. *J. Am. Chem. Soc.* **1993**, *115*, 7328.

33 Song, H. K.; Palmore, G. T. R. *Adv. Mater.* **2006**, *18*, 1764.

34 Beer, P. D.; Kocian, O.; Mortimer, R. J.; Ridgway, C. *Analyst* **1992**, *117*, 1247.

35 Der, B. S.; Dattelbaum, J. D. *Anal. Biochem.* **2008**, *375*, 132.

36 Reuillard, B.; Le Goff, A.; Cosnier, S. *Chem. Commun.* **2014**, *50*, 11731.

37 Chia, J. S. Y.; Tan, M. T.; Khiew, P. S.; Chin, J. K.; Siong, C. W. *Sensor. Actuator. B-Chem.* **2015**, *210*, 558.

38 Jang, H.; Lee, J.; Min, D.-H. *J. Mater. Chem. B* **2014**, *2*, 2452.

39 Milton, R. D.; Minteer, S. D. *J. Electrochem. Soc.* **2014**, *161*, H3011.

40 Lei, Y.; Chen, W.; Mulchandani, A. *Anal. Chim. Acta* **2006**, *568*, 200.

41 Wang, J.; Sun, X. W.; Wei, A.; Lei, Y.; Cai, X.; Li, C. M.; Dong, Z. L. *Appl. Phys. Lett.* **2006**, *88*, 3106.

42 Karyakin, A. A.; Gitelmacher, O. V.; Karyakina, E. E. *Anal. Chem.* **1995**, *67*, 2419.

43 Wang, B.; Li, B.; Deng, Q.; Dong, S. *Anal. Chem.* **1998**, *70*, 3170.

44 Ghica, M. E.; Brett, C. *Electroanalysis* **2006**, *18*, 748.

45 Revzin, A. F.; Sirkar, K.; Simonian, A.; Pishko, M. V. *Sensor. Actuator. B-Chem.* **2002**, *81*, 359.

46 Abayomi, L. A.; Terry, L. A.; White, S.; Warner, P. *Biosens. Bioelectron.* **2006**, *21*, 2176.

47 Moser, I.; Jobst, G.; Urban, G. A. *Biosens. Bioelectron.* **2002**, *17*, 297.

48 Sprules, S. D.; Hart, J. P.; Pittson, R.; Wring, S. A. *Electroanalysis* **1996**, *8*, 539.

49 Cui, X.; Li, C. M.; Zang, J.; Yu, S. *Biosens. Bioelectron.* **2007**, *22*, 3288.

50 Young, D. G.; Holroyd, J. D.; Hall, P. F. *Biochem. Biophys. Res. Commun.* **1970**, *38*, 184.

51 Sigel, H. *Angew. Chem. Int. Edit.* **1969**, *8*, 167.

52 Jansen, E. F.; Olson, A. C. *Arch. Biochem. Biophys.* **1969**, *129*, 221.

53 Sassolas, A.; Blum, L. J.; Leca-Bouvier, B. D. *Biotechnol. Adv.* **2012**, *30*, 489.

54 Singhal, R.; Gambhir, A.; Pandey, M.; Annapoorni, S.; Malhotra, B. *Biosens. Bioelectron.* **2002**, *17*, 697.

55 Liu, G.; Lin, Y. *Electrochem. Commun.* **2006**, *8*, 251.

56 Wang, J.; Wang, L.; Di, J.; Tu, Y. *Talanta* **2009**, *77*, 1454.

57 Parente, A.; Marques, E.; Azevedo, W.; Diniz, F.; Melo, E.; Lima Filho, J. *Appl. Biochem. Biotechnol.* **1992**, *37*, 267.

58 Dhand, C.; Das, M.; Datta, M.; Malhotra, B. *Biosens. Bioelectron.* **2011**, *26*, 2811.

59 Sangodkar, H.; Sukeerthi, S.; Srinivasa, R.; Lal, R.; Contractor, A. *Anal. Chem.* **1996**, *68*, 779.

60 Kan, J.; Pan, X.; Chen, C. *Biosens. Bioelectron.* **2004**, *19*, 1635.

61 Arora, K.; Sumana, G.; Saxena, V.; Gupta, R. K.; Gupta, S.; Yakhmi, J.; Pandey, M.; Chand, S.; Malhotra, B. *Anal. Chim. Acta* **2007**, *594*, 17.

62 Tembe, S.; Inamdar, S.; Haram, S.; Karve, M.; D'Souza, S. *J. Biotechnol.* **2007**, *128*, 80.

63 Tembe, S.; Karve, M.; Inamdar, S.; Haram, S.; Melo, J.; D'Souza, S. F. *Anal. Biochem.* **2006**, *349*, 72.

64 Bartlett, P.; Whitaker, R. *J. Electroanal. Chem. Interfacial Electrochem.* **1987**, *224*, 27.

65 Rubianes, M. a. D.; Rivas, G. A. *Electrochem. Commun.* **2003**, *5*, 689.

66 Cosnier, S.; Lambert, F.; Stoytcheva, M. *Electroanalysis* **2000**, *12*, 356.

67 Shan, D.; Cosnier, S.; Mousty, C. *Biosens. Bioelectron.* **2004**, *20*, 390.

68 De Melo, J.; Cosnier, S.; Mousty, C.; Martelet, C.; Jaffrezic-Renault, N. *Anal. Chem.* **2002**, *74*, 4037.

69 Migneault, I.; Dartiguenave, C.; Bertrand, M. J.; Waldron, K. C. *Biotechniques* **2004**, *37*, 790.

70 López-Gallego, F.; Betancor, L.; Mateo, C.; Hidalgo, A.; Alonso-Morales, N.; Dellamora-Ortiz, G.; Guisán, J. M.; Fernández-Lafuente, R. *J. Biotechnol.* **2005**, *119*, 70.

71 Fernandez-Lafuente, R.; Rosell, C.; Rodriguez, V.; Guisan, J. *Enzyme Microb. Technol.* **1995**, *17*, 517.

72 Malhotra, B. D.; Chaubey, A. *Sensor. Actuator. B-Chem.* **2003**, *91*, 117.

73 Ramanathan, K.; Pandey, S. S.; Kumar, R.; Gulati, A.; Murthy, A. S. N.; Malhotra, B. D. *J. Appl. Polym. Sci.* **2000**, *78*, 662.

74 Fabbrini, M.; Galli, C.; Gentili, P. *J. Mol. Catal. B: Enzym.* **2002**, *16*, 231.

75 Ivnitski, D.; Atanassov, P. *Electroanalysis* **2007**, *19*, 2307.

76 Giroud, F.; Minteer, S. D. *Electrochem. Commun.* **2013**, *34*, 157.

77 Meredith, M. T.; Minson, M.; Hickey, D.; Artyushkova, K.; Glatzhofer, D. T.; Minteer, S. D. *ACS Catal.* **2011**, *1*, 1683.

78 Werlen, C.; Jaspers, M. C.; van der Meer, J. R. *Appl. Environ. Microbiol.* **2004**, *70*, 43.

79 Rainina, E.; Efremenco, E.; Varfolomeyev, S.; Simonian, A.; Wild, J. *Biosens. Bioelectron.* **1996**, *11*, 991.

80 Zlatev, R.; Magnin, J.-P.; Ozil, P.; Stoytcheva, M. *Biosens. Bioelectron.* **2006**, *21*, 1493.

81 Milton, R. D.; Wang, T.; Knoche, K. L.; Minteer, S. D. *Langmuir* **2016**, *32*, 2291.

82 Mulchandani, A.; Chen, W.; Mulchandani, P.; Wang, J.; Rogers, K. R. *Biosens. Bioelectron.* **2001**, *16*, 225.

83 Mulchandani, P.; Mulchandani, A.; Kaneva, I.; Chen, W. *Biosens. Bioelectron.* **1999**, *14*, 77.

84 Kara, S.; Keskinler, B.; Erhan, E. *J. Chem. Technol. Biotechnol.* **2009**, *84*, 511.

85 Timur, S.; Anik, U.; Odaci, D.; Gorton, L. *Electrochem. Commun.* **2007**, *9*, 1810.

86 Neufeld, T.; Biran, D.; Popovtzer, R.; Erez, T.; Ron, E. Z.; Rishpon, J. *Anal. Chem.* **2006**, *78*, 4952.

87 Zlatev, R. K.; Stoytcheva, M. S.; Salas, B. V.; Magnin, J.-P.; Ozil, P. *Electrochem. Commun.* **2006**, *8*, 1699.

88 Germain, M. N.; Arechederra, R. L.; Minteer, S. D. *J. Am. Chem. Soc.* **2008**, *130*, 15272.

89 Wang, T.; Reid, R. C.; Minteer, S. D. *Electroanalysis* **2015**, *28,* 854.

90 Moehlenbrock, M. J.; Meredith, M. T.; Minteer, S. D. *ACS Catal.* **2011**, *2*, 17.

91 Giroud, F.; Nicolo, T. A.; Koepke, S. J.; Minteer, S. D. *Electrochim. Acta* **2013**, *110*, 112.

92 Rasmussen, M.; Minteer, S. D. *Anal. Methods* **2013**, *5*, 1140.

93 Emily, H.-Y. C.; Wei, M. C.; Weiler, S.; Flavell, R. A.; Mak, T. W.; Lindsten, T.; Korsmeyer, S. J. *Molecular Cell* **2001**, *8*, 705.

94 Letai, A.; Bassik, M. C.; Walensky, L. D.; Sorcinelli, M. D.; Weiler, S.; Korsmeyer, S. J. *Cancer Cell* **2002**, *2*, 183.

95 Cheng, E. H.-Y.; Sheiko, T. V.; Fisher, J. K.; Craigen, W. J.; Korsmeyer, S. J. *Science* **2003**, *301*, 513.

96 Zhao, J.; Meng, F.; Zhu, X.; Han, K.; Liu, S.; Li, G. *Electroanalysis* **2008**, *20*, 1593.

97 Maltzman, S. L.; Minteer, S. D. *Anal. Methods* **2012**, *4*, 1202.

98 Rousset, S.; Alves-Guerra, M.-C.; Mozo, J.; Miroux, B.; Cassard-Doulcier, A.-M.; Bouillaud, F.; Ricquier, D. *Diabetes* **2004**, *53*, S130.

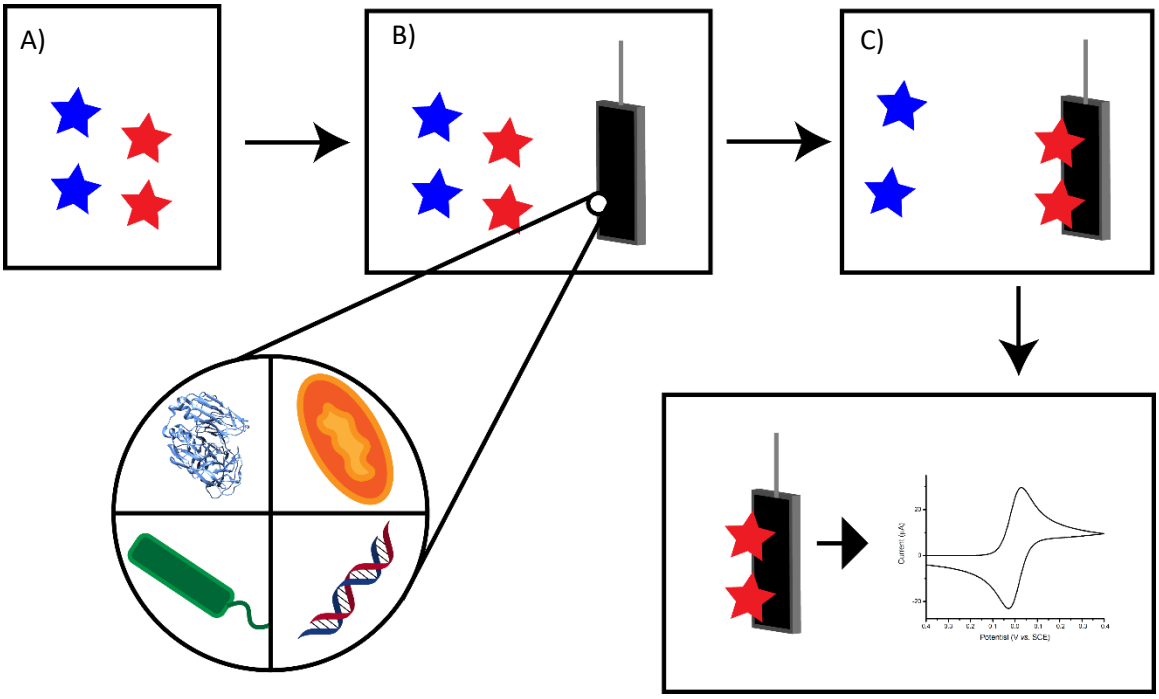

Figure 1.1: Flow chart of biosensing process, A) a system contains analyte and interference components, B) those components interact with the biosensor, C) the biosensor recognizes the analyte, D) the transducer generates a signal.

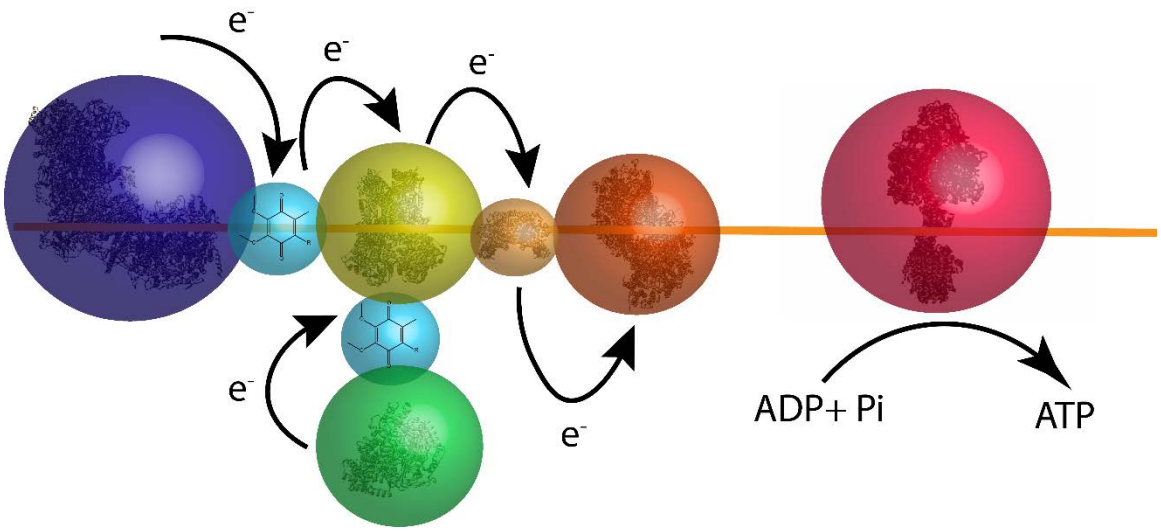

Figure 1.2: Structure of mitochondrial electron transport chain, showing mitochondrial inner membrane (yellow line), mitochondrial complex I (purple), complex II (green), complex III (yellow), complex IV (orange), complex V (red), ubiquinone (cyan), and cytochrome c (brown).

CHAPTER 2

LACCASE INHIBITION BY ARSENITE/ARSENATE: DETERMINATION OF INHIBITION MECHANISM AND PRELIMINARY APPLICATION TO A SELF-POWERED BIOSENSOR

In this chapter, the reversible inhibition of laccase by arsenite (As^{3+}) and arsenate (As^{5+}) is reported. Oxygen-reducing laccase bioelectrodes were found to be inhibited by both arsenic species for direct electron-transfer bioelectrodes (using anthracene functionalities for enzymatic orientation) and for mediated electron-transfer bioelectrodes [using 2,2'-azino-bis(3-ethylbenzothiazoline-6-sulfonic acid) (ABTS) as an electron mediator]. Both arsenic species were determined to behave via a mixed inhibition model (behaving closely to that of uncompetitive inhibitors) when evaluated spectrophotometrically using ABTS as the electron donor. Finally, laccase biocathodes were employed within an enzymatic fuel cell, yielding a self-powered biosensor for arsenite and arsenate. This conceptual self-powered arsenic biosensor demonstrated limit of detection (LODs) of 13 µM for arsenite and 132 µM for arsenate. Further, this device

Reprinted (adapted) with permission from Analytical Chemistry 88.6 (2016): 3243-3248.

possessed sensitivities of 0.91 ± 0.07 mV/mM for arsenite and 0.98 ± 0.02 mV/mM for arsenate.

2.1 Introduction

Arsenic is a commonly occurring groundwater pollutant largely originating from mines, industrial waste and other natural processes.[1-2] Arsenic is present in the environment in both organic and inorganic forms. Among polluting inorganic arsenic species, arsenate and arsenite are the most common and toxic forms in groundwater,[3] therefore their environmental monitoring is necessary. Electrochemical monitoring of arsenic in water has been extensively studied and different electrochemical techniques have been evaluated for their suitability of detecting arsenic in environmental samples, such as polarography,[4-5] and cathodic or anodic stripping voltammetry.[6-7] Electrochemical detection techniques for arsenic have been transplanted to microarray platforms aimed at portable and field-deployable sensing purposes as opposed to high sensitivity applications (such as spectroscopic and chromatographic techniques), where portability is often troublesome.[8-9]

Electrochemical arsenic sensors typically consist of a three-electrode system including a working, reference and counter electrode. A potentiostat is required to input energy into the cell and regulate the sensor. Additionally, a three-electrode device is bulky, which is unfavorable for field applications and technologies. In this paper, we aim to transition to self-powered systems for arsenic sensing.

An enzymatic fuel cell (EFC) utilizes enzymes as biocatalytic alternatives to commonly used metal catalysts, such as platinum. EFCs are compact two-electrode systems that generate power. Self-powered biosensors based on EFC technology thus do not require an external electrical energy source.[10-22] Previous studies on self-powered biosensors have demonstrated that they are able to be fueled or inhibited by an analyte.[23-28] EFCs that are fueled by glucose have been extensively reported[29-31] and some have been extended to self-powered biosensors.[32-34] A large number of glucose/O_2 EFCs utilize laccase as the cathodic biocatalyst for O_2 reduction to H_2O.[33,35-40] Herein, we report the first experimental evidence of the enzymatic inhibition of laccase by both arsenite and arsenate (Figure 2.1). The enzymatic inhibition model was elucidated using ABTS as a substrate for colorimetric assays. Further, laccase was combined with flavin adenine dinucleotide-dependent glucose dehydrogenase (FAD-GDH) to yield a glucose/O_2 EFC that is able to operate as a self-powered biosensor for arsenate and arsenite detection.

2.2 Experimental

2.2.1 Chemicals and materials

FAD-dependent glucose dehydrogenase (FAD-GDH) was purchased from Sekesui Diagnostics (U.K.) and used as received. Toray carbon paper was purchased from Fuel Cell Earth (U.S.A.) and used as received. Hydroxyl-functionalized multiwalled carbon nanotubes were purchased from Cheaptubes and used as received. Tetrabutylammonium bromide modified Nafion (TBAB-

Nafion) was prepared based on a previously reported procedure.[41] All other chemicals were purchased from Sigma-Aldrich (reagent grade) and used as received.

2.2.2 Laccase and FAD-GDH bioelectrodes fabrication

Both laccase and FAD-GDH bioelectrodes are fabricated based on previously published procedures. Laccase biocathode is fabricated based on the following procedure: 20 mg/mL laccase in pH 5.5 citrate-phosphate buffer was mixed with 100 mg/mL anthracene-functionalized multiwalled carbon nanotube (Ac-MWCNT) and vortex-mixed for a total of 4 min along with sonication for a total of 1 min.[41] The resulting mixture was then mixed with 25% v/v TBAB-Nafion, vortex-mixed for an additional minute, and sonicated for an additional 15 s. Then approximately 33 µL of the mixture is applied to a 1 cm^2 square of Toray carbon paper via a brush and dried at room temperature before evaluation.

For the FAD-GDH bioanode fabrication, dimethyferrocene-functionlized linear poly(ethylenimine) ($FeMe_2$-LPEI) was synthesized and FAD-GDH bioanode were prepared, as previously reported.[42] The FAD-GDH bioanodes were prepared by mixing 10 mg/mL ferrocene redox polymer, 30 mg/mL FAD-GDH and 10% v/v ethylene glycol diglycidyl ether (EGDGE) in a ratio of 56:24:3. A 10 µL aliquot of the mixture was applied to a 0.25 cm^2 Toray paper electrode surface and dried for 12 h at room temperature. Electrodes were rinsed immediately before use.

2.2.3 UV-Vis assay for determining laccase inhibition mechanism

UV-Vis kinetic assays were performed on a BioTex Synergy HTX multiplate reader. The absorbance of ABTS oxidation was monitored at 420 nm with different substrate concentrations (500, 100, 40, 20, 10, 4 µM). The concentrations of arsenite and arsenate tested were 0.5, 1, 2, 4, 8, 12 mM, and the concentration of laccase was 13 µg/mL. All tests were performed in citrate-phosphate buffer (200 mM pH 5.5).

2.2.4 Electrochemical measurements

A three-electrode configuration was used for cyclic voltammetry and amperometric *i–t* experiments. A saturated calomel electrode (SCE) was used as the reference electrode, and a platinum mesh was used as the counter electrode. Enzymatic fuel cells were evaluated by galvanostatically drawing increasing current at a slow ramp rate (0.1 µA/s) until short circuit. The self-powered biosensor was evaluated by continuously drawing 10% of its maximum current density of the enzymatic fuel cell and monitoring the potential difference with increasing concentrations of arsenite and arsenate. All experiments were performed at 22 ± 1 °C.

2.3 Results and discussion

2.3.1 Determination of laccase inhibition reversibility

Laccase is known to be able to undergo both mediated (MET) and direct electron transfer.[43-47] Laccase bioelectrodes were prepared with Ac-MWCNTs to

orientate the type I copper center of laccase toward the electrode surface.[48] This favorable orientation results in DET of laccase, yielding a bioelectrode that is able to undergo the direct bioelectrocatalytic reduction of O_2 to H_2O (Figure 2.2).

The reversibility of arsenite and arsenate inhibition to laccase was firstly investigated by evaluation of laccase bioelectrodes in buffer (in the absence of arsenate and arsenite). Immersion of a laccase bioelectrode in buffer that contains dissolved O_2 results in a catalytic reductive wave, due to the direct bioelectrocatalytic reduction of O_2 to H_2O by laccase (onset potential of approximately +600 mV vs SCE). The addition of arsenite or arsenate yields a decreased catalytic response for O_2 reduction, due to enzyme inhibition. Replacing the buffer with arsenite/arsenate-free buffer returns the catalytic current generated by O_2 reduction to approximately 100%, demonstrating the reversibility of the inhibition mechanism.

2.3.2 Determination of laccase inhibition mechanism of arsenite and arsenate via UV-Vis colorimetric assay

After electrochemically determining the reversibility of laccase inhibition by arsenate and arsenite, UV-Vis colorimetric assays were performed utilizing ABTS as electron donor. An apparent rate versus arsenite and arsenate is presented in Figure 2.3. As shown in Figure 2.3, the increasing of arsenite or arsenate concentration (from 0 to 12 mM) leads to decrease of the maximum apparent reaction rate (V_{max}) from 1.02 ± 0.08 to 0.13 ± 0.00 abs/min for arsenite and 1.16 ± 0.06 to 0.66 ± 0.04 abs/min for arsenate; a detailed description of the V_{max} value under different concentration of arsenite and arsenate is shown in Table 2.1.

Additionally, the Michaelis constant (K_M) also decreases, which is indicative of an uncompetitive inhibition mechanism.[48-49] To further elucidate the inhibition mechanism, Lineweaver-Burk double-reciprocal plots were evaluated for differing concentrations of each inhibitor, as shown in Figure 2.4. A convergence of data sets on the Y-axis of Lineweaver-Burk plots is typical of a competitive inhibition mechanism, while convergence of related data sets on the X-axis is indicative of a non-competitive inhibition mechanism. Analysis of the Lineweaver-Burk double-reciprocal plots indicate a mixed inhibition model (incorporating both uncompetitive and noncompetitive inhibition models), although the nonlinear regression performed above suggest the inhibition model lay nearer to that of an uncompetitive inhibition model. The K_i value for laccase inhibition by arsenic was determined for a mixed inhibition model (by nonlinear regression), with 2.3 ± 1.4 mM reported for arsenite and 15.4 ± 10.1 mM reported for arsenate. R^2 values for individual Michaelis-Menten fittings are reported in Table 2.2. An uncompetitive inhibition model fit by nonlinear regression yielded overall R^2 values of 0.9617 for arsenate and 0.9420 for arsenite (n = 3).

2.3.3 Laccase inhibition monitored by amperometry

Subsequently, amperometric i-t analysis (Figure 2.5) was performed at 0.2 V (vs. SCE) with consecutive injections of either arsenate or arsenite. At this potential, O_2 is reduced to H_2O by the laccase biocathodes. Following the introduction of oxygen into the nitrogen-purged buffer, a catalytic current is observed corresponding to the direct bioelectrocatalytic of reduction of oxygen by laccase. With each subsequent injection of arsenite or arsenate, a decrease in

catalytic current is observed with arsenite/arsenate concentrations ranging from 0.5 to 11 mM. The corresponding catalytic currents decrease for the laccase biocathodes in the range of 5-90% current for arsenite and 2-30% current for arsenate. The laccase bioelectrodes exhibited sensitivities of 46.9 ± 7.0 and 10.6 ± 1.2 μA/mM for arsenite and arsenate, respectively. Their corresponding linear dynamic ranges were approximately 0.5 – 5 mM arsenite (R^2 = 0.9923) and 0.5 - 8 mM arsenate (R^2 = 0.9894).

Finally, additional amperometric experiments were performed to further elucidate the enzymatic inhibition model, as shown in Figure 2.6. Laccase bioelectrodes were prepared in the absence of anthracene functionalities on the MWCNTs (to eliminate DET contributions), and enzymatic bioelectrocatalysis was facilitated with injections of ABTS as the electron mediator and substrate (under constant O_2 concentrations) in the presence of arsenite (Figure 2.6A) and arsenate (Figure 2.6B). R^2 values for multiple inhibition models applied to this data by nonlinear regression fits are presented in Table 2.3, where mixed inhibition models had the greatest correlation for both inhibitors.

2.3.4 Self-Powered laccase arsenite and arsenate sensor

Following the determination of the inhibition mechanism for laccase, previously-reported FAD-GDH bioanodes (incorporating a ferrocene redox polymer for MET) were coupled with laccase biocathodes (undergoing DET), yielding glucose/O_2 EFCs operating on 100 mM glucose.[42] The bioanodes and biocathodes were prepared on Toray carbon paper electrodes, with the biocathodes as the limiting components (for enhanced arsenite/arsenate

sensitivity). Figure 2.7 demonstrates the mediated bioelectrocatalytic oxidation of glucose by FAD-GDH, where the presence of arsenite and arsenate do not affect enzymatic activity. Figure 2.8A presents a polarization and resulting power curve for the glucose/O_2 EFC, in the absence and presence of arsenite/arsenate. EFCs were evaluated galvanostatically, by drawing gradually increasing current from the EFC until short circuit (ramp rate of 1 μA/s). The EFCs possessed open circuit potentials (OCPs) of 723.3 ± 4.5 mV. The maximum current and power densities were 289.7 ± 12.4 μA cm^{-2} and 57.2 ± 1.9 μW cm^{-2} (mean ± standard deviation, n = 3).

As a self-powered sensor that does not require any external energy source to operate, only 10% of the maximum current is drawn from the glucose/O_2 EFC and the potential difference is monitored as a function of time (Figure 2.8 B and C). With 10% of the maximum current withdrawn from the biofuel cell, it can be seen that the biofuel cell retains approximately 73% of its OCP. Successive aliquots of arsenite or arsenate are injected into the electrolyte/buffer/fuel solution, which results in a decrease in potential difference of the EFC. For arsenite or arsenate at a final concentration of 1-20 mM, a decrease in the potential difference of the EFC of 20 mV is observed. To eliminate variation between each EFC, the percentage change of the initial OCP of EFC is averaged and plotted.

Differences in the inhibitory effects of arsenic for the self-powered EFC experiments and the amperometric laccase experiments are due to the experimental conditions employed (potentiostatic and galvanostatic), where galvanostatic experiments are continuously changing the potential of the

bioelectrode. The continuously changing potential difference between the T1 Cu site of laccase and the electrode architecture continuously alters the catalytic turnover of the bioelectrodes and, by default, alters the effects of the inhibitors at the bioelectrodes.[51]

2.4 Conclusion

In conclusion, this chapter reports the enzymatic inhibition of laccase and laccase bioelectrodes (DET type) by both arsenite and arsenate, for which a mixed (with preference to uncompetitive inhibition) inhibition model was determined by UV-Vis spectrophotometric assays. The laccase biocathodes were then employed within a glucose/O_2 EFC, yielding a self-powered arsenite/arsenate biosensor. The device possessed LODs of 13 µM for arsenite and 132 µM for arsenate, with sensitivities of 0.91 ± 0.07 mV/mM for arsenite and 0.98 ± 0.02 mV/mM for arsenate, capable of detecting acute arsenite and arsenate poisoning.[52] Linear dynamic ranges for the EFCs were evaluated for 1 – 20 mM arsenite (R^2 = 0.9934) and 1 – 8 mM arsenate (R^2 = 0.9810). Further, the device only operated at 10% current draw of the maximum current density of the EFC.

While this conceptual study demonstrates how the inhibition of laccase and laccase bioelectrodes by arsenite and arsenate can yield a self-powered biosensor for their detection, future studies will address the suitability of this system in actual field samples as well as develop an array system to investigate the possible effect of other contaminants on the self-powered biosensor (i.e. fluoride). Interference from chloride is expected to minimal, because the use of anthracene as an

orientation moiety has been demonstrated to be able to out-compete chloride inhibition (which acts as a competitive inhibitor).[53]

2.5 References

1 McArthur, J.; Ravenscroft, P.; Safiulla, S.; Thirlwall, M. *Water Resour. Res.* **2001**, *37*, 109-117.

2 Berg, M.; Stengel, C.; Trang, P. T. K.; Viet, P. H.; Sampson, M. L.; Leng, M.; Samreth, S.; Fredericks, D. *Sci. Total Environ.* **2007**, *372*, 413-425.

3 Hughes, M. F. *Toxicol. Lett.* **2002**, *133*, 1-16.

4 Reyes-Salas, E.; Dosal-Gomez, M.; Barcelo-Quintal, M.; Manzanilla-Cano, J. *Anal. Lett.* **2002**, *35*, 123-133.

5 Sharma, P. *Anal. Sci.* **1995**, *11*, 261-262.

6 Li, H.; Smart, R. B. *Anal. Chim. Acta* **1996**, *325*, 25-32.

7 Adeloju, S.; Young, T. *Anal. Lett.* **1997**, *30*, 147-161.

8 Tercier-Waeber, M. L.; Pei, J.; Buffle, J.; Fiaccabrino, G.; Koudelka-Hep, M.; Riccardi, G.; Confalonieri, F.; Sina, A.; Graziottin, F. *Electroanalysis* **2000**, *12*, 27-34.

9 Nolan, M. A.; Kounaves, S. P. *Anal. Chem.* **1999**, *71*, 3567-3573.

10 Sekretaryova, A. N.; Beni, V.; Eriksson, M.; Karyakin, A. A.; Turner, A. P.; Vagin, M. Y. *Anal. Chem.* **2014**, *86*, 9540-9547.

11 Li, Z.; Rosenbaum, M. A.; Venkataraman, A.; Tam, T. K.; Katz, E.; Angenent, L. T. *Chem. Commun.* **2011**, *47*, 3060-3062.

12 Zhou, M.; Zhou, N.; Kuralay, F.; Windmiller, J.; Parkhomovsky, S.; Valdes-Ramirez, G.; Katz, E.; Wang, J. *Angew. Chem. Int. Ed.* **2012**, *51*, 2686-2689.

13 Cheng, J.; Han, Y.; Deng, L.; Guo, S. *Anal. Chem.* **2014**, *86*, 11782-11788.

14 Sekretaryova, A. N.; Beni, V.; Eriksson, M.; Karyakin, A. A.; Turner, A. P. F.; Vagin, M. Y. *Anal. Chem.* **2014**, *86*, 9540-9547.

15 Hou, C.; Fan, S.; Lang, Q.; Liu, A. *Anal. Chem.* **2015**, *87*, 3382-3387.

16 Pinyou, P.; Conzuelo, F.; Sliozberg, K.; Vivekananthan, J.; Contin, A.; Pöller, S.; Plumeré, N.; Schuhmann, W. *Bioelectrochemistry* **2015**, *106, Part A*, 22-27.

17 Zhou, M. *Electroanalysis* **2015**, *27*, 1786-1810.

18 Kang, Z.; Gu, Y.; Yan, X.; Bai, Z.; Liu, Y.; Liu, S.; Zhang, X.; Zhang, Z.; Zhang, X.; Zhang, Y. *Biosens. Bioelectron.* **2015**, *64*, 499-504.

19 Strambini, L. M.; Longo, A.; Scarano, S.; Prescimone, T.; Palchetti, I.; Minunni, M.; Giannessi, D.; Barillaro, G. *Biosens. Bioelectron.* **2015**, *66*, 162-168.

20 Zhao, Y.; Fu, Y.; Wang, P.; Xing, L.; Xue, X. *Nanoscale* **2015**, *7*, 1904-1911.

21 Jia, X.; Dong, S.; Wang, E. *Biosens. Bioelectron.* **2016**, *76*, 80-90.

22 Sode, K.; Yamazaki, T.; Lee, I.; Hanashi, T.; Tsugawa, W. *Biosens. Bioelectron.* **2016**, *76*, 20-28.

23 Zhang, L.; Zhou, M.; Dong, S. *Anal. Chem.* **2012**, *84*, 10345-10349.

24 Wen, D.; Deng, L.; Guo, S.; Dong, S. *Anal. Chem.* **2011**, *83*, 3968-3972.

25 Conzuelo, F.; Vivekananthan, J.; Pöller, S.; Pingarrón, J. M.; Schuhmann, W. *ChemElectroChem* **2014**, *1*, 1854-1858.

26 Deng, L.; Chen, C.; Zhou, M.; Guo, S.; Wang, E.; Dong, S. *Anal. Chem.* **2010**, *82*, 4283-4287.

27 Wen, D.; Deng, L.; Guo, S.; Dong, S. *Anal. Chem.* **2011**, *83*, 3968-3972.

28 Deng, L.; Chen, C.; Zhou, M.; Guo, S.; Wang, E.; Dong, S. *Anal. Chem.* **2010**, *82*, 4283-4287.

29 Sakai, H.; Nakagawa, T.; Tokita, Y.; Hatazawa, T.; Ikeda, T.; Tsujimura, S.; Kano, K. *Energy Environ. Sci.* **2009**, *2*, 133-138.

30 Cinquin, P.; Gondran, C.; Giroud, F.; Mazabrard, S.; Pellissier, A.; Boucher, F.; Alcaraz, J. P.; Gorgy, K.; Lenouvel, F.; Mathe, S.; Porcu, P.; Cosnier, S. *PLoS One* **2010**, *5*, e10476

31 Mano, N.; Mao, F.; Heller, A. *J. Am. Chem. Soc.* **2003**, *125*, 6588-6594.

32 Meredith, M. T.; Minteer, S. D. *Analytical Chemistry* **2011**, *83*, 5436-5441.

33 Katz, E.; Bückmann, A. F.; Willner, I. *J. Am. Chem. Soc.* **2001**, *123*, 10752-10753.

34 Newman, J. D.; Turner, A. P. *Biosens. Bioelectron.* **2005**, *20*, 2435-2453.

35 Barrière, F.; Kavanagh, P.; Leech, D. *Electrochim. Acta* **2006**, *51*, 5187-5192.

36 Brunel, L.; Denele, J.; Servat, K.; Kokoh, K. B.; Jolivalt, C.; Innocent, C.; Cretin, M.; Rolland, M.; Tingry, S. *Electrochem. Commun.* **2007**, *9*, 331-336.

37 Mano, N.; Mao, F.; Heller, A. *J. Am. Chem. Soc.* **2003**, *125*, 6588-6594.

38 Barrière, F.; Ferry, Y.; Rochefort, D.; Leech, D. *Electrochem. Commun.* **2004**, *6*, 237-241.

39 Scodeller, P.; Carballo, R.; Szamocki, R.; Levin, L.; Forchiassin, F.; Calvo, E. J. *J. Am. Chem. Soc.* **2010**, *132*, 11132-11140.

40 Gallaway, J. W.; Barton, S. A. C. *J. Electroanalysis Chem.* **2009**, *626*, 149-155.

41 Meredith, M. T.; Minson, M.; Hickey, D.; Artyushkova, K.; Glatzhofer, D. T.; Minteer, S. D. *ACS Catalysis* **2011**, *1*, 1683-1690.

42 Milton, R. D.; Lim, K.; Hickey, D. P.; Minteer, S. D. *Bioelectrochemistry* **2015**, *106*, 56-63.

43 Milton, R. D.; Minteer, S. D. *J. Electrochem. Soc.* **2014**, *161*, H3011-H3014.

44 Shleev, S.; Jarosz-Wilkolazka, A.; Khalunina, A.; Morozova, O.; Yaropolov, A.; Ruzgas, T.; Gorton, L. *Bioelectrochemistry* **2005**, *67*, 115-124.

45 Shleev, S.; Tkac, J.; Christenson, A.; Ruzgas, T.; Yaropolov, A. I.; Whittaker, J. W.; Gorton, L. *Biosens. Bioelectron.* **2005**, *20*, 2517-2554.

46 Kuznetsov, B.; Shumakovich, G.; Koroleva, O.; Yaropolov, A. *Biosens. Bioelectron.* **2001**, *16*, 73-84.

47 Riva, S. *Trends Biotechnol.* **2006**, *24*, 219-226.

48 Meredith, M. T.; Minson, M.; Hickey, D.; Artyushkova, K.; Glatzhofer, D. T.; Minteer, S. D. *ACS Catal*. **2011**, *1*, 1683-1690.

49 Cornish-Bowden, A. *Biochem. J* **1974**, *137*, 143-144.

50 Lineweaver, H.; Burk, D. *J. Am. Chem. Soc.* **1934**, *56*, 658-666.

51 Amine, A.; Alafandy, M.; Kauffmann, J. M.; Pekli, M. N. *Anal. Chem.* **1995**,

67, 2822-2827.

52 Ratnaike, R. N. *Postgrad. Med. J.* **2003**, *79*, 391-396.

53 Milton, R. D.; Giroud, F.; Thumser, A. E.; Minteer, S. D.; Slade, R. C. *Chem. Commun.* **2014**, *50*, 94-96.

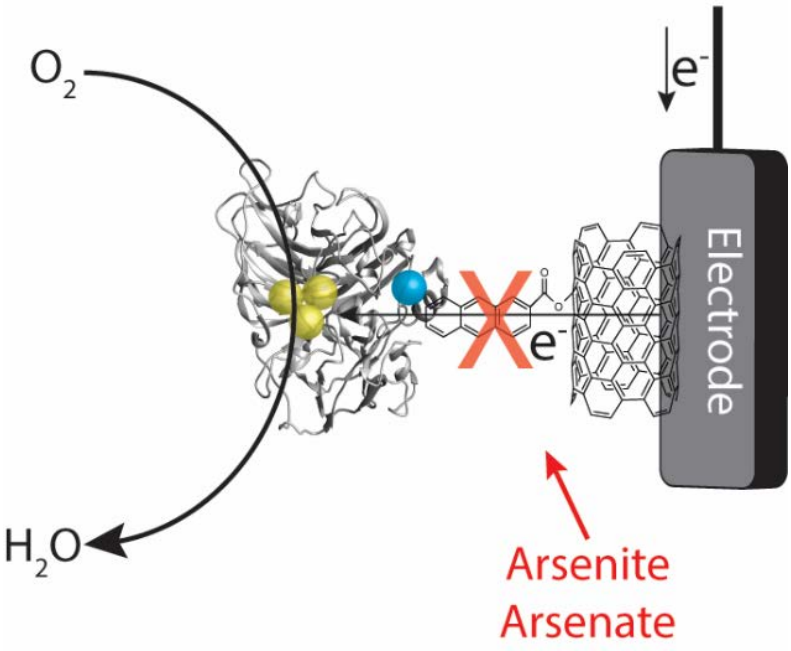

Figure 2.1: Direct electron-transfer-type laccase bioelectrodes are inhibited by arsenite and arsenate.

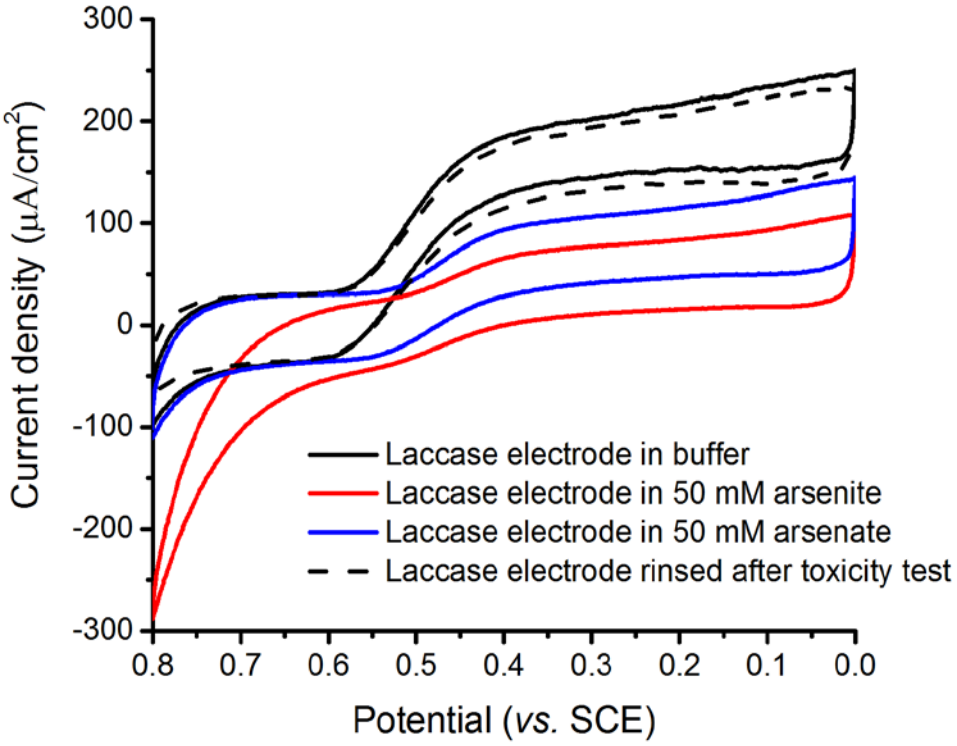

Figure 2.2: Representative cyclic voltammograms of laccase bioelectrodes in citrate-phosphate buffer (200 mM, pH 5.5, stirred) in the presence of 50 mM arsenate (blue line) or 50 mM arsenite (red line). Inhibited laccase bioelectrodes were rinsed and evaluated in fresh citrate-phosphate buffer (representative data set presented as dashed black line for As^{3+} and As^{5+} inhibited bioelectrodes). All electrodes were evaluated at a scan rate of 10 mV/s.

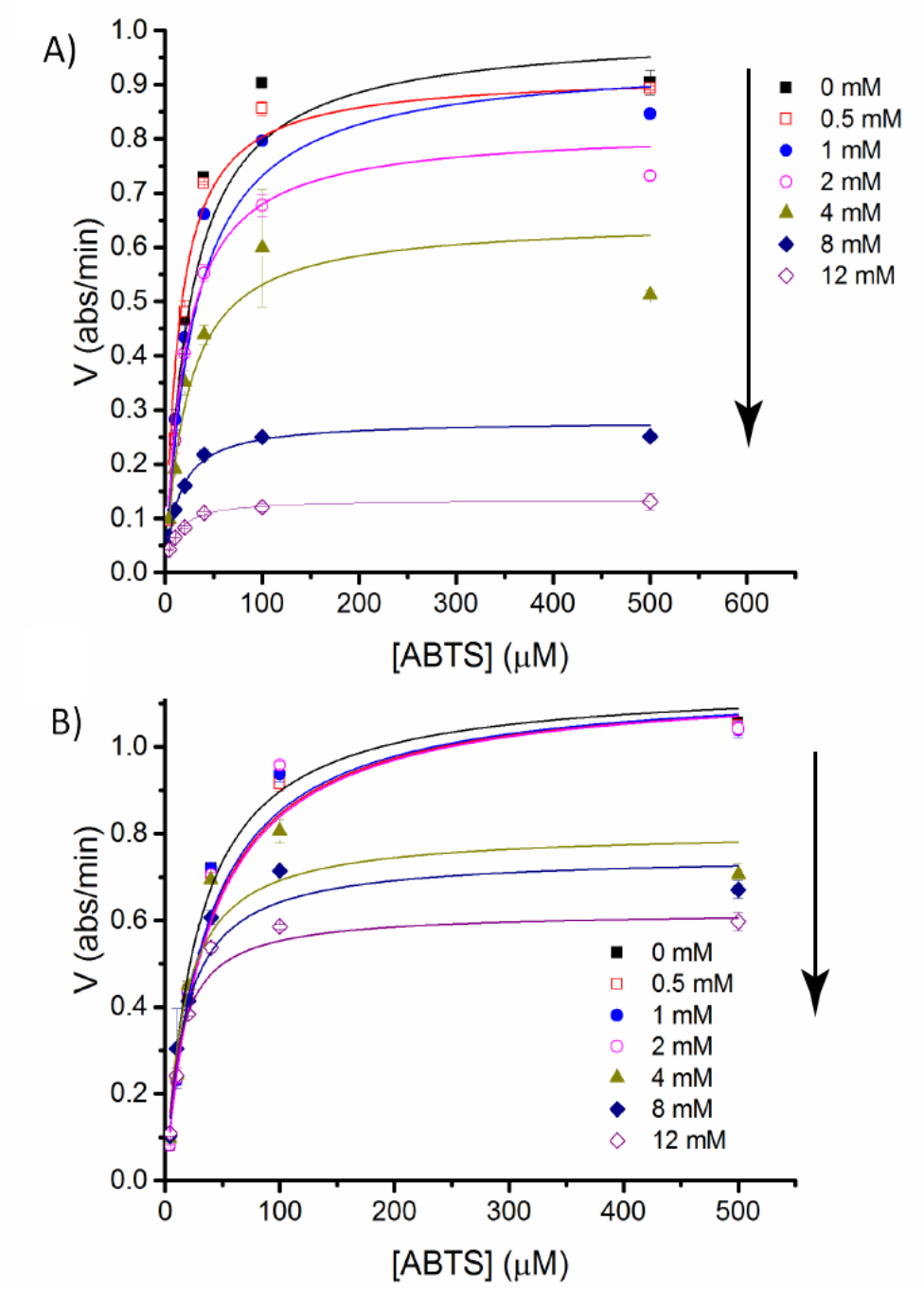

Figure 2.3: Spectroscopic determination of apparent Michaelis-Menten kinetics for the reduction of ABTS with different concentrations of A) arsenite or B) arsenate present. Kinetics were determined at pH 5.5, by following the enzymatic oxidation of ABTS.

A)

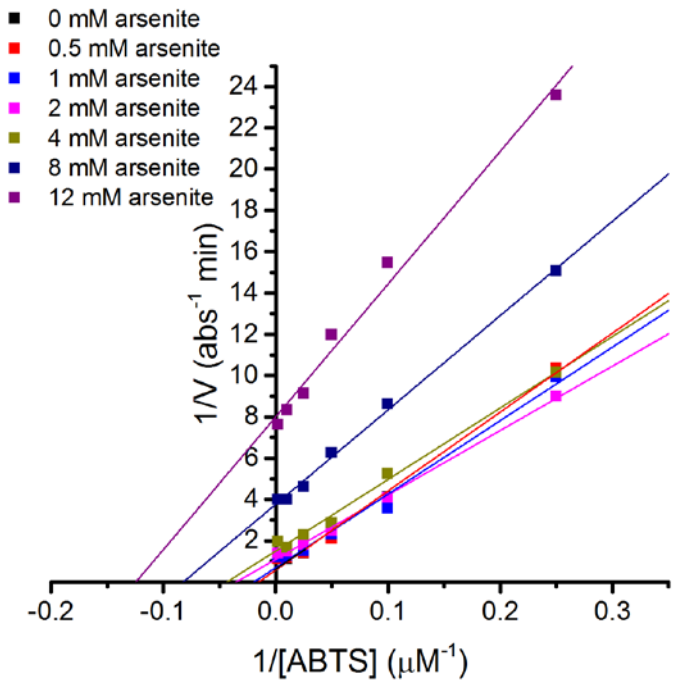

B)

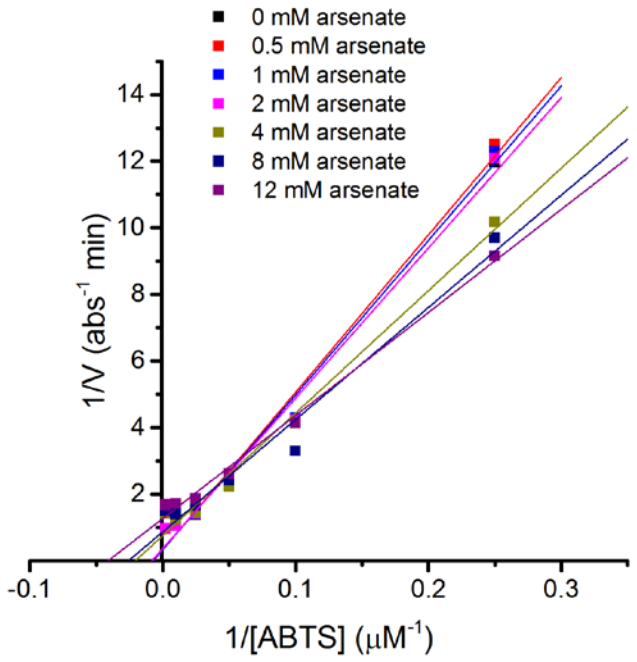

Figure 2.4: Lineweaver-Burk double reciprocal plot of the reduction of O_2 by laccase, monitored by following the absorbance of ABTS in citrate-phosphate buffer with differing concentrations of A) arsenite and B) arsenate. Data presented as mean (n=3).

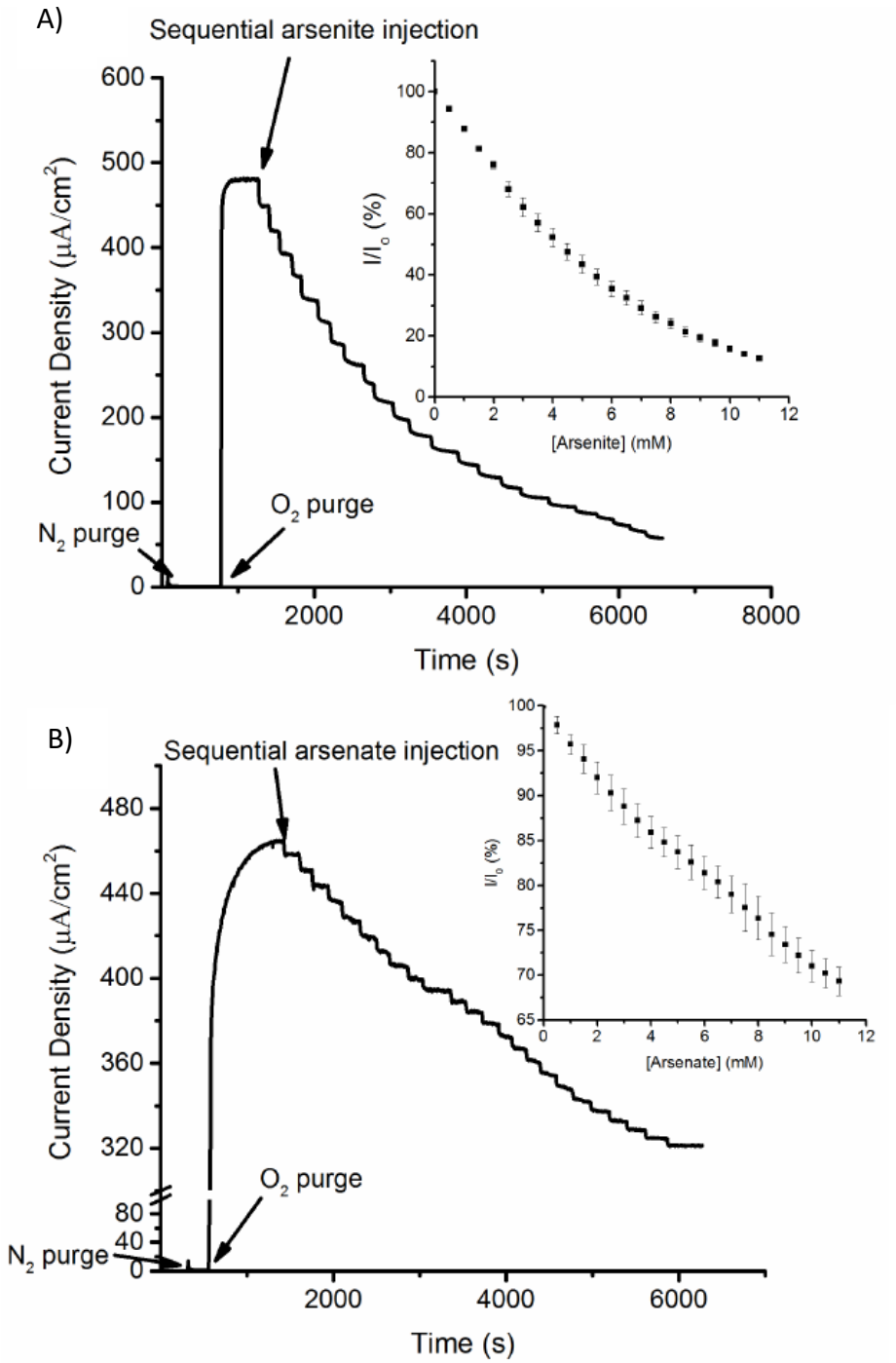

Figure 2.5: Representative amperometric *i*-t curves of laccase bioelectrodes with successive injections of A) arsenite and B) arsenate. (Inset figure: Averaged percentage change of each laccase electrode with injections of A) arsenite and B) arsenate). Experiments were performed at pH 5.5 (200 mM citrate-phosphate buffer), under hydrodynamic (stirred) conditions.

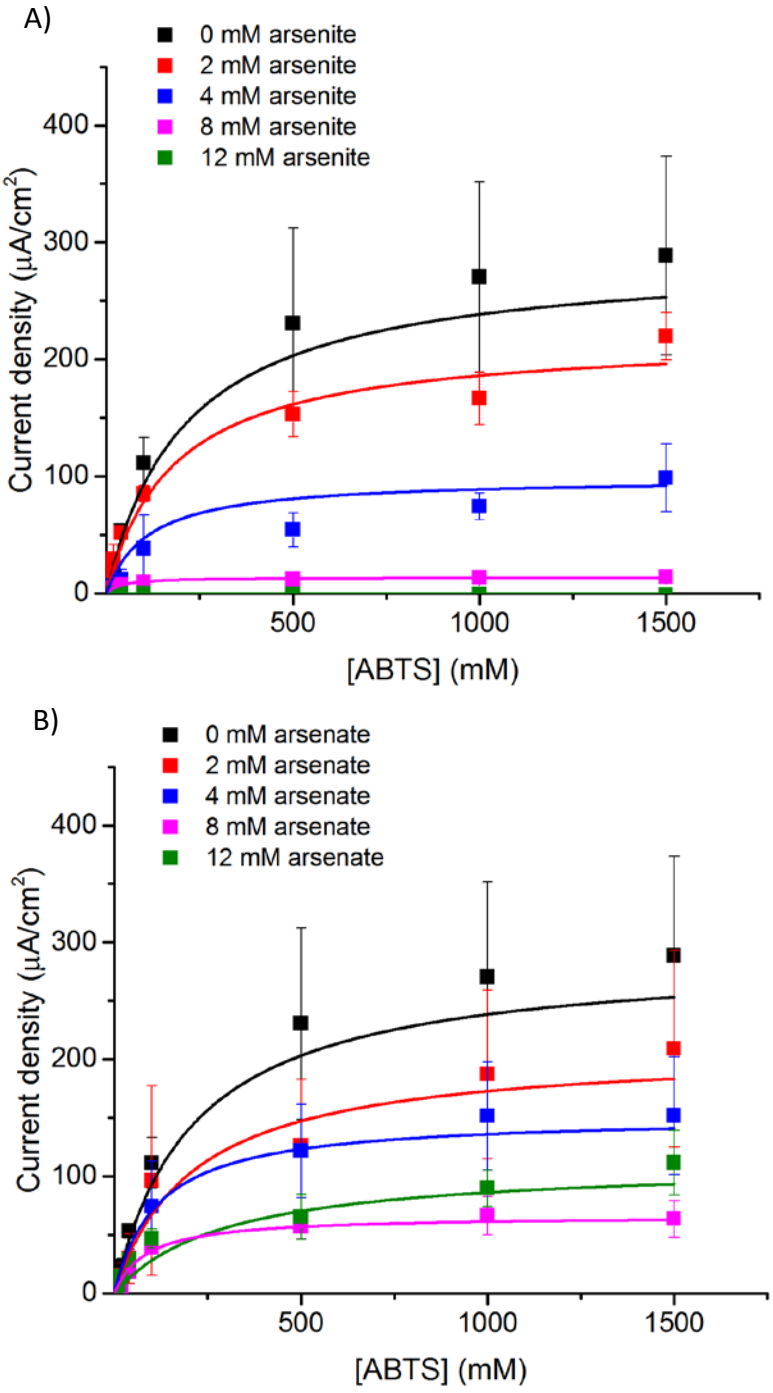

Figure 2.6: Apparent Michealis-Menten kinetics of laccase determined via amperometry at 0 V vs. SCE using ABTS as substrate at different A) arsenite and B) arsenate concentrations. Electrochemical measurements were conducted in 200 mM phosphate-citrate buffer at pH 5.5.

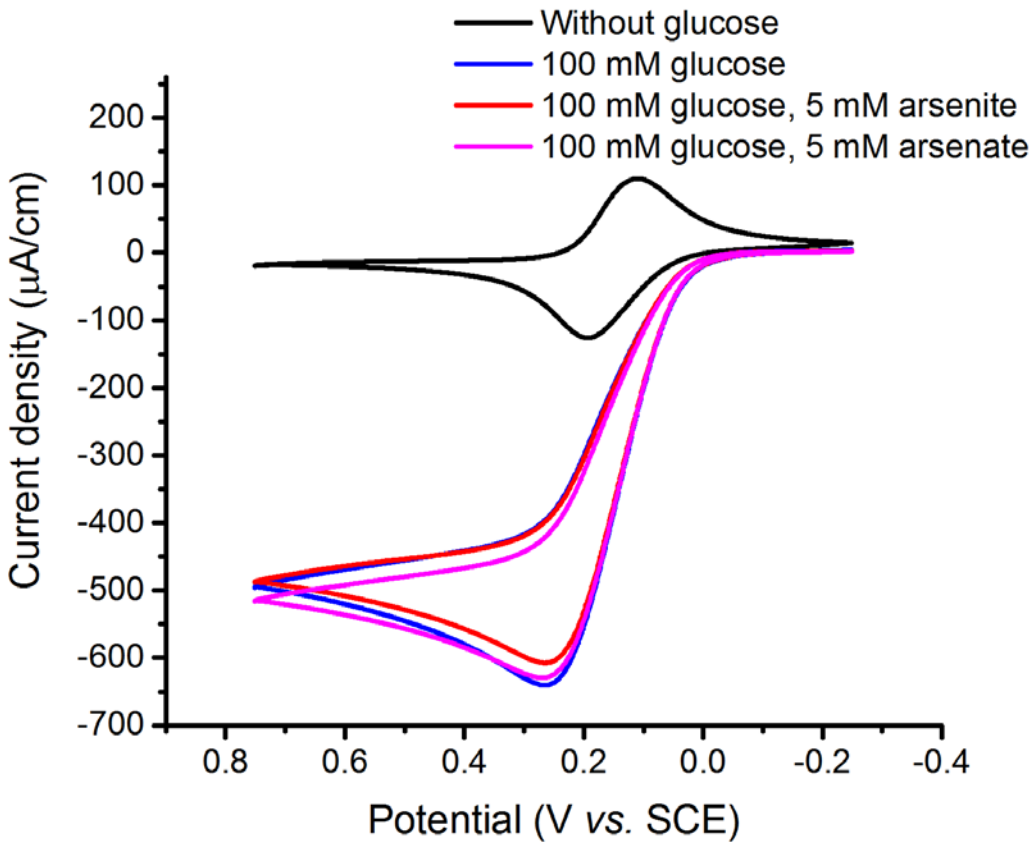

Figure 2.7: Representative cyclic voltammograms of FAD-GDH bioanodes in citrate-phosphate buffer (pH 5.5, 200 mM) without glucose (black line), with 100 mM glucose (blue line), with 100 mM glucose and 5 mM arsenite (red line), and with 100 mM glucose and arsenate (blue line).

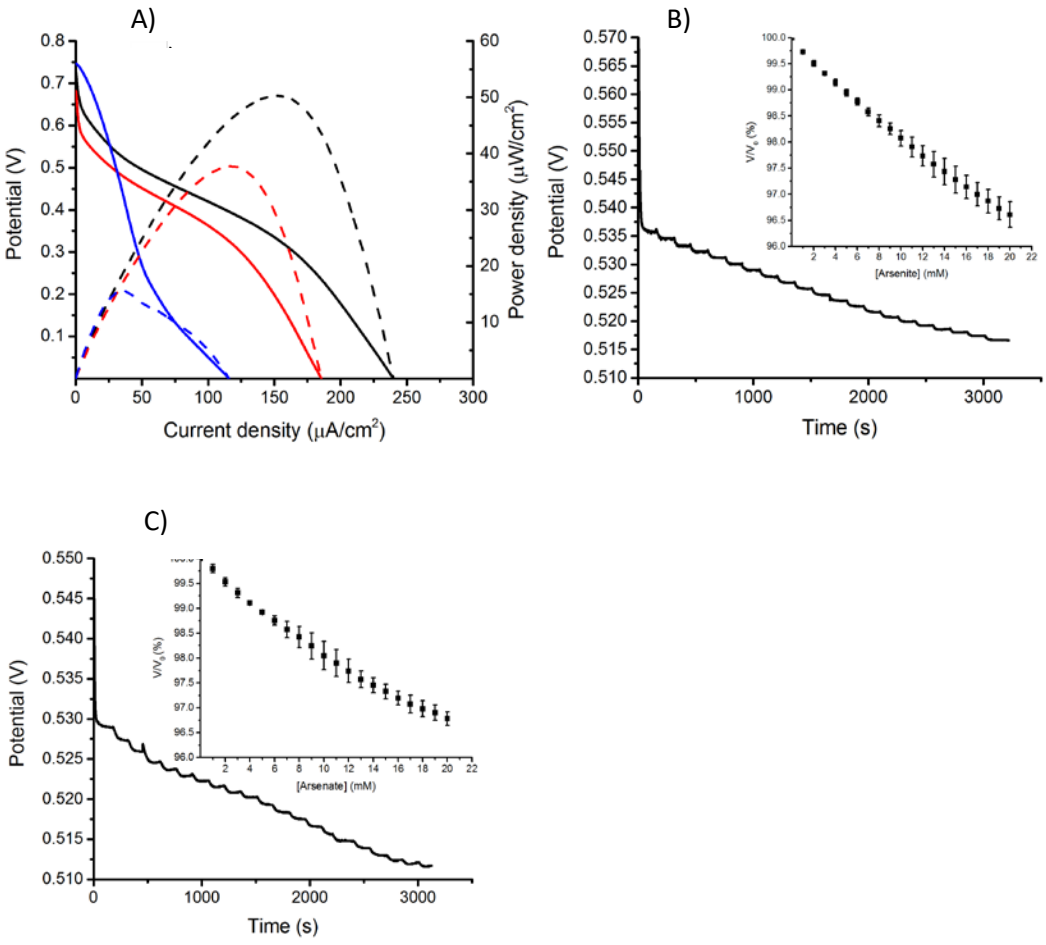

Figure 2.8: A) Representative polarization curve for a glucose/O_2 EFC (black solid line), operating in citrate-phosphate buffer (pH 5.5, 200 mM, stirred) containing 100 mM glucose. Corresponding power curves are presented as dashed lines. EFCs were also operated in the presence of 20 mM arsenite (red lines) and 20 mM arsenate (blue lines). B) Representative chronopotentiometric traces for EFCs operating at 10% current draw with sequential injections of 1 mM arsenite. C) Representative chronopotentiometric traces for EFCs operating at 10% current draw with sequential injections of 1 mM arsenate. Inset graphs present the averaged percentage change of the EFCs' potential differences with arsenic injections. Error bars represent standard deviation (*n* = 3).

Table 2.1: V_{max} and K_m values of O_2 reduced by laccase monitored by following the absorbance of ABTS in citrate-phosphate buffer, the data are obtained with nonlinear regression fitting.

[Arsenite]	**0 mM**	**0.5 mM**	**1 mM**	**2 mM**	**4 mM**	**8 mM**	**12 mM**
$V_{max\ (mol/min)}$	1.02 ± 0.08	0.99 ± 0.07	0.92 ± 0.04	0.78 ± 0.02	0.59 ± 0.05	0.27 ± 0.01	0.13 ± 0.0
$K_{m\ (mM)}$	23.2 ± 5.7	21.7 ± 4.9	21.3 ± 3.5	19.7 ± 2.1	15.8 ± 5.1	12.6 ± 1.6	10.2 ± 1.0
[Arsenate]	**0 mM**	**0.5 mM**	**1 mM**	**2 mM**	**4 mM**	**8 mM**	**12 mM**
$V_{max\ (mol/min)}$	1.16 ± 0.06	1.15 ± 0.06	1.15 ± 0.07	1.15 ± 0.07	0.93 ± 0.09	0.77 ± 0.05	0.66 ± 0.04
$K_{m\ (mM)}$	31.4 ± 5.2	32.6 ± 5.2	30.6 ± 5.6	30.3 ± 5.5	21.3 ± 6.4	15.6 ± 3.8	14.9 ± 2.9

Table 2.2: R^2 values for the nonlinear regression fitting of laccase activity monitored by UV under different concentrations of arsenite and arsenate.

[Arsenite]	**0**	**0.5**	**1**	**2**	**4**	**8**	**12**
R^2	0.9317	0.9635	0.9635	0.9499	0.8358	0.2593	0.9557
[Arsenate]	**0**	**0.5**	**1**	**2**	**4**	**8**	**12**
R^2	0.9787	0.9801	0.9774	0.9620	0.8710	0.9330	0.9624

Table 2.3: Global R^2 values retrieved from Michealis-Menten nonlinear regression fits for laccase under differing inhibition models for arsenite or arsenate.

Inhibition model	Arsenite	Arsenate
Mixed inhibition	**0.8424**	**0.8065**
Uncompetitive inhibition	0.8310	0.8029
Noncompetitive inhibition	0.8423	0.8060
Competitive inhibition	0.8187	0.7757

CHAPTER 3

A PAPER-BASED MITOCHONDRIAL ELECTROCHEMICAL BIOSENSOR FOR PESTICIDE DETECTION

In this chapter, we detail a paper-based three-electrode electrochemical biosensor using a mitochondria modified Toray carbon paper working electrode. Cyclic voltammetry performed on the paper-based biosensor and similar electrodes in a common laboratory setup (not in an integrated paper-based device) compare favorably. In addition, instant detection of malathion with a detection limit of 20 nM by cyclic voltammetry is demonstrated, showing the device can potentially be used as a portable platform for pesticides detection.

3.1 Introduction

The increasing use of pesticides rises a significant environmental problem, and is threatening human health via acute poisoning and long-term carcinogenic effects. [1] Pesticide detection plays an important role in mitigating the negative consequences of pesticide contamination. Many different pesticide detection techniques have previously been developed, with chromatographic techniques being the most widely used. [2] Although those methods have exhibited

outstanding sensitivity (usually at the ng/ ml concentration level), they require expensive, bulky instrumentation not readily available in many parts of the world. An inexpensive, small, portable pesticide detection system would therefore be very useful in preventing harmful pesticide effects.

Up till now, many low cost and disposable enzymatic or microbial paper-based sensors have been reported utilizing different detection methods such as optical methods, [3] colorimetric methods [4] and electrochemical methods. [5] Recently, electrochemical sensors have been extensively studied because of their great potential as a portable sensor.

Electrochemical sensors have a rapid response time and can be operated using compact ubiquitous devices such as smart phones. [6] Many enzymatic electrochemical pesticide biosensors have been studied including those using the enzymes alkaline phosphatase, [7] acetylcholinesterase (AchE), [8] glucose oxidase[9] and organophosphate hydrolase. [10] These enzymatic biosensors either act via enzymatic inhibition or directly use organophosphate pesticides as a substrate, and they have shown good sensitivity and low detection limits. Some of those electrochemical sensors utilized a microfluidic or portable platform.

Different platforms have been used for electrochemical detection, and among those different platforms paper-based devices stand out because of their ultra-low materials cost. In addition, paper utilizes capillary flow to move fluid samples so external pumping is not required, which further decreases device cost and complexity. These advantages, combined with the fact that paper-based devices can be produced via roll-to-roll fabrication methods, make them suitable

for large-scale production.

For organophosphate pesticide detection, AchE is extensively studied [11] and shows an outstanding low detection limit to many different organophosphate pesticides such as malathion (detection limit 100 nM), [12] parathion (detection limit 130 pM) [13] and paraoxon (detection limit 1 nM). [14] However, as a universal pesticide sensor, AchE is only capable of detecting neurotoxic pesticides, primarily organophosphate and carbamate pesticides, which are inhibitors of cholinesterase enzymes. Other pesticides function on completely different mechanisms, for instance, by blocking sodium channels, inhibiting cytochrome oxidase or interfering with DNA/RNA synthesis. [15] Therefore, in terms of universality, using an organelle or even a whole cell has a clear advantage over a single-enzyme assay, because they are generically sensitive to all toxic pesticides. As organelles, thylakoids and mitochondria have been tested against different pesticides via electrochemical methods and showed capability of detecting those pesticides at concentrations below an environmentally safe level. [5]

Mitochondria are the organelles responsible for respiration and ATP synthesis. As shown in Figure 3.1, a previous study showed that the mitochondrial electron transport chain (ETC) contains electrochemical active species, like quinones, that are able to communicate with carbon electrodes, therefore allowing electrochemical monitoring of mitochondrial health. [16] For most pesticides, mitochondria are their primary or secondary target. [15] In previous studies, mitochondria have been tested against many different

pesticides like atrazine, parathion, paraquat and permethrin. [5a] It is notable that a mitochondrial biosensor can detect not only neurotoxins, but also many non-neurotoxic pesticides, unlike an AchE based biosensor, therefore making it ideal for detecting a variety of pesticides. Since mitochondria produce a different electrochemical output in response to different toxins, it may be possible to distinguish between toxins using a single sensor.

In this work, we demonstrate that a mitochondrial biosensor can be utilized in a paper-based platform. Malathion was used as a test case for evaluating the biosensor sensitivity and detection limit. The results are comparable to a typical enzymatic malathion sensor, which illustrates the paper-based mitochondrial biosensor's potential as a portable pesticide sensor. [12]

3.2. Experimental

3.2.1 Isolation of mitochondria from bovine heart

Mitochondria were isolated from fresh bovine heart based using a slightly modified procedure from Rogers *et al*. [17] The bovine heart were cut into 3 cm cubes and disrupted with a blender in MHSE buffer (70 mM sucrose, 210 mM mannitol, 5 mM HEPES, 1 mM EGTA, 0.5 % (w/v) BSA, pH 7.2), followed by adjusting the pH back to near neutral, and isolating mitochondria via gradient centrifugation. In this process, the disrupted meat was first centrifuged at 26,000 g for 10 min, then the pellet was resuspended and centrifuged at 500 g for 10 min and repeated again. This process was followed by filtering the mitochondria pellet with cheese cloth, then centrifuging at 10000 g for 10 min twice and finally suspending in 300 mM trehalose solution, as described in previous literature. [18]

3.2.2 Assembling of the paper-based mitochondrial biosensor

Toray carbon paper (TGP-H-060, FuelCell Earth, non-wet-proof) was chosen as the electrode material for the working and counter electrodes due to its large surface area. The Toray carbon paper electrodes were laser cut to a designated shape shown in Figure 3.2.

The circular regions on the working and counter electrodes measured 3 mm and 5 mm in diameter, respectively. These areas were modified with mitochondria and platinum as described below to become the electrochemically active electrode surfaces while the remaining electrodes' surfaces were used for fluid and electrical conduction. The paper-based sample strip was created by using vinyl tape to mask a circular region on a piece of Whatman filter paper and then manually coating the unmasked areas with wax. The wax was melted on a hot plate and the mask was removed. A laser-cut polyester envelope with a circular hole in it for pipetting the sample was fabricated and used to contain the sensor components and thus increase the robustness of this device.

3.2.3 Electrode modification and electrochemistry test

Aliquots containing 7 mg of mitochondria in trehalose solution were drop cast on the Toray carbon paper working electrode and dried in air at room temperature. A thin layer of silica was vapor deposited onto the mitochondria using tetramethyl orthosilicate (TMOS) as previously described. [19] Platinum was electrochemically deposited on the Toray paper counter electrode using a 1 :7 (v/v) Pt-Pb mixture in PBS (137 mM NaCl, 2.7 mM KCl, 10 mM Na_2HPO_4,

1.8 mM KH_2PO_4, 1 mM $CaCl_2$, 0.5 mM $MgCl_2$), and cycling from 200 to -700 mV (vs. Ag/AgCl) at a scan rate of 50 mV/s for 25 cycles. The reference electrode was fabricated by curing silver epoxy on a piece of filter paper. After curing, the filter paper was cut into 2 mm wide strips and oxidized in 3 M $FeCl_3$ solution for 1 minute to generate a AgCl layer on the surface of the silver epoxy. Then, an agar layer with 3.5 M KCl was deposited on the surface of the electrode as a salt bridge. [20] Unless otherwise noted, electrochemical experiments were carried out by cyclic voltammetry with a potential range from 600 to -600 mV vs. Ag/AgCl at a scan rate of 20 mV/s, in 100 mM pH 7.2 phosphate-nitrate buffer containing 1 mM EGTA and 5% BSA.

3.3 Results and discussion

3.3.1 Mitochondrial biosensor cyclic voltammetry *in vitro* and on the paper-based chip

Mitochondria are considered the powerhouse of the living cell, because they contain a variety of metabolic pathways, including the Krebs cycle and the ETC. Mitochondria can communicate with an electrode via the electrochemically active species inside its ETC. One of the electrochemically active species in the ETC that is accessible through the membrane is quinone, which is believed to be the means of mitochondrial communication with the electrode. This was previously verified in our group by testing mitochondria from various biologically sources on Toray paper with their quinone pool depleted. This led to total removal of all mitochondrial peaks, revealing that quinone is the most probable electrochemically active species that is communicating with the electrode. [16]

Figure 3.3 shows the cyclic voltammogram of a bovine heart mitochondria modified electrode in 100 mM pyruvate in phosphate-nitrate buffer. The mitochondrial voltammogram shows an oxidation peak around 100 mV vs. Ag/AgCl and a reduction peak around -300 mV. The same peaks are also observed in the mitochondrial voltammogram on the paper-based chip, suggesting that the chip platform has a very similar electrochemical response in a portable platform. The small reduction peak at 0 V is commonly observed on Toray paper and is more noticeable on the blue curve due to the increased electrode size. It is noticeable that with smaller electrodes, mitochondria on the paper-based chip showed a smaller peak current, which is likely because of the different mitochondria loading density. Another difference between the mitochondrial electrodes on the paper-based chip and the common 3-electrode lab setup is that the potential difference between the oxidation peak and reduction peak is smaller on the paper-based chip. This can be explained by the higher mitochondrial loading density on the paper-based electrode, which leads to a lower diffusion coefficient.

3.3.2 Mitochondrial inhibition by pesticides

Many pesticides, such as parathion, permethrin and paraquat, target mitochondria and inhibit the different complexes in the mitochondrial ETC. [5a] Previously, mitochondria inhibition has been most commonly observed by measuring its oxygen consumption rate with the addition of different kinds of pesticides, which indicates a decrease in mitochondria metabolism. [21]

Mitochondrial electrochemistry is a direct method to monitor mitochondrial health, and it is potentially more efficient than measuring oxygen consumption, because tests can be performed directly in ambient air.

When mitochondria are exposed to different toxins, different complexes inside the mitochondrial ETC are inhibited, e.g. permethrin inhibits complex I, [22] carboxin inhibits complex II, [23] cyanide inhibits complex IV [24] and malathion inhibits complex II and IV. [21] Previous work in our group showed that mitochondrial electrodes behave differently when they are exposed to different environmental toxins. [5a] Because of the structure of the ETC and since the different complexes inside the mitochondrial ETC play different roles in quinone redox chemistry, inhibition of different complexes inside the mitochondrial ETC will lead to different types of electrochemical responses. For instance, the inhibition of complex I would theoretically lead to a decrease of the mitochondrial oxidative peak and an increase of the mitochondrial reductive peak, while inhibition of complex III would lead to removal of all mitochondrial peaks due to the complete shutting down of mitochondrial ETC. In addition, for healthy mitochondria, the response often consists of two parts: the uncoupling effect and inhibition of mitochondrial complexes in the ETC.

Uncoupling begins when mitochondria are isolated from cells. During the uncoupling process, the mitochondrial membrane’s permeability increases leading to a loss of the proton gradient between mitochondrial intermembrane space and matrix. [25] Therefore, the activity of mitochondrial ETC complexes increases to compensate for such change. The combination of the increase of

mitochondrial membrane permeability and the increase of mitochondrial ETC metabolic level induces an increase of mitochondrial oxidation and reduction currents. [26] From Figure 3.4b, it can be seen that when mitochondria are uncoupled, both the oxidative peak and the reductive peak current, as well as the capacitance increase significantly. It can be also seen that when mitochondria are exposed to malathion, as shown in Figure 3.4a, the type of response is similar to uncoupling, while different to examples where mitochondria are exposed to complex II or V inhibitors, where a decrease of signal is observed.

It was reported previously that malathion is an inhibitor for mitochondrial complex II and IV, as well as a mitochondrial uncoupler. [27] The increase of both the oxidation and reduction peaks is likely caused by mitochondrial uncoupling rather than ETC inhibition, which would manifest itself by increasing either the oxidation or reduction peak, but not both. Therefore, while uncoupling and ETC inhibition may both be occurring, for malathion, the uncoupling effect dominates the electrochemical response. Mitochondrial uncoupling happens after mitochondria are isolated from cells regardless of their exposure to toxins. To exclude the effect of time-dependent mitochondrial uncoupling, a control group used a mitochondrial-modified electrode similar to the one used for the experimental group, instead of blank carbon paper.

Cyclic voltammetry was performed on the paper-based sensor at increasing malathion concentrations and in the absence of and presence of 100 mM pyruvate (as shown in Figure 3.1). With the addition of malathion, the mitochondrial oxidation and reduction peaks both increase.

Figure 3.5 shows the mitochondrial oxidative peak current change when exposed to different concentrations of malathion and the mitochondrial oxidative peak change over time without malathion. There was no noticeable mitochondria uncoupling when electrodes are stored in cold environments. It can therefore be concluded that oxidative peak current changes are due to malathion exposure. Although this mitochondrial biosensor showed concentration dependency with malathion, this sensor was originally design as an on-off threshold sensor with a 20 nM limit of detection at the 98% confidence level.

3.4 Conclusions

In this paper, we successfully miniaturized mitochondrial electrochemistry for use on a paper-based chip that was simple to fabricate and easy to use. The paper-based labon-a-chip device was capable of detecting malathion above concentrations of 20 nM. Due to its limit of detection and ease of use, this device shows promise as a portable sensor. Given mitochondrial sensitivity to a variety of pesticides and the potential ability to distinguish them, similar paper-based mitochondrial biosensors could be used as versatile electrochemical testing platforms for other pesticides as well.

3.5 References

1 D. D. Weisenburger, *Hum. Pathol.* **1993**, *24*, 571-576.

2 a) S. Schachterle, R. D. Brittain, J. D. Mills, *J. Chromatogr. A* **1994**, *683*, 185-193; b) N. Brito, S. Navickiene, L. Polese, E. Jardim, R. Abakerli, M. Ribeiro, *J. Chromatogr. A* **2002**, *957*, 201-209.

3 a) J. Kumar, S. K. Jha, S. D'Souza, *Biosens. Bioelectron.* **2006**, *21*, 2100-2105; b) A. Mulchandani, P. Mulchandani, I. Kaneva, W. Chen, *Anal. Chem.* **1998**, *70*, 4140-4145; c) A. Mulchandani, W. Chen, P. Mulchandani, J. Wang, K. R. Rogers, *Biosens. Bioelectron.* **2001**, *16*, 225-230.

4 a) S. Z. Hossain, R. E. Luckham, M. J. McFadden, J. D. Brennan, *Anal. Chem.* **2009**, *81*, 9055-9064; b) S. Z. Hossain, J. D. Brennan, *Anal. Chem.* **2011**, *83*, 8772-8778; c) S. Z. Hossain, R. E. Luckham, A. M. Smith, J. M. Lebert, L. M. Davies, R. H. Pelton, C. D. Filipe, J. D. Brennan, *Anal. Chem.* **2009**, *81*, 5474-5483.

5 a) S. L. Maltzman, S. D. Minteer, *Anal. Methods* **2012**, *4*, 1202-1206; b) M. Rasmussen, S. D. Minteer, *Anal. Methods* **2013**, *5*, 1140-1144; c) J.-C. Chen, J.-L. Shih, C.-H. Liu, M.-Y. Kuo, J.-M. Zen, *Anal. Chem.* **2006**, *78*, 3752-3757.

6 a) X. Wang, M. R. Gartia, J. Jiang, T.-W. Chang, J. Qian, Y. Liu, X. Liu, G. L. Liu, *Sensor. Actuat. B-Chem.* **2015**, *209*, 677-685; b) A. Nemiroski, D. C. Christodouleas, J. W. Hennek, A. A. Kumar, E. J. Maxwell, M. T. Fernández-Abedul, G. M. Whitesides, *P. Natl. Acad. Sci.* **2014**, *111*, 11984-11989.

7 F. Mazzei, F. Botrè, S. Montilla, R. Pilloton, E. Podestà, C. Botrè, *J. Electroanal. Chem.* **2004**, *574*, 95-100.

8 D. Du, X. Ye, J. Cai, J. Liu, A. Zhang, *Biosens. Bioelectron.* **2010**, *25*, 2503-2508.

9 C. Malitesta, M. Guascito, *Biosens. Bioelectron.* **2005**, *20*, 1643-1647.

10 a) C. M.-H. Cho, A. Mulchandani, W. Chen, *Protein Eng. Des. Sel.* **2006**, *19*, 99-105; b) V. Sacks, I. Eshkenazi, T. Neufeld, C. Dosoretz, J. Rishpon, *Anal. Chem.* **2000**, *72*, 2055-2058; c) A. Sahin, K. Dooley, D. M. Cropek, A. C. West, S. Banta, *Sensor. Actuat. B-Chem.* **2011**, *158*, 353-360.

11 a) H. Zhao, X. Ji, B. Wang, N. Wang, X. Li, R. Ni, J. Ren, *Biosens. Bioelectron.* **2015**, *65*, 23-30; b) A. Apilux, C. Isarankura-Na-Ayudhya, V. Prachayasittikul, T. Tantinongcolwat, *Exp. Clin. Sci. J.* **2015**, *14*, 307-319; c) Q. Long, H. Li, Y. Zhang, S. Yao, *Biosens. Bioelectron.* **2015**, *68*, 168-174.

12 A. Hart, W. Collier, D. Janssen, *Biosens. Bioelectron.* **1997**, *12*, 645-654.

13 P. Raghu, T. M. Reddy, B. K. Swamy, B. Chandrashekar, K. Reddaiah, M. Sreedhar, *J. Electroanal. Chem.* **2012**, *665*, 76-82.

14 T. T. Bachmann, R. D. Schmid, *Anal. Chim. Acta* **1999**, *401*, 95-103.

15 J. E. Casida, *Chem. Res. Toxicol.* **2009**, *22*, 609-619.

16 F. Giroud, T. A. Nicolo, S. J. Koepke, S. D. Minteer, *Electrochim. Acta* **2013**, *110*, 112-119.

17 G. W. Rogers, M. D. Brand, S. Petrosyan, D. Ashok, A. A. Elorza, D. A. Ferrick, A. N. Murphy, *PloS one* **2011**, *6*, e21746.

18 R. Yamaguchi, A. Andreyev, A. Murphy, G. Perkins, M. Ellisman, D. Newmeyer, *Cell Death Differ.* **2007**, *14*, 616-624.

19 H. R. Luckarift, S. R. Sizemore, J. Roy, C. Lau, G. Gupta, P. Atanassov, G. R. Johnson, *Chem. Commun.* **2010**, *46*, 6048-6050.

20 H. Suzuki, H. Shiroishi, S. Sasaki, I. Karube, *Anal. Chem.* **1999**, *71*, 5069-5075.

21 E. H. Delgado, E. L. Streck, J. L. Quevedo, F. Dal-Pizzol, *Neurochem. Res.* **2006**, *31*, 1021-1025.

22 B. Gassner, A. Wüthrich, G. Scholtysik, M. Solioz, *J. Pharmacol. Exp. Ther.* **1997**, *281*, 855-860.

23 H. Miyadera, K. Shiomi, H. Ui, Y. Yamaguchi, R. Masuma, H. Tomoda, H. Miyoshi, A. Osanai, K. Kita, S. Ōmura, *P. Natl. A. Sci.* **2003**, *100*, 473-477.

24 J. Alonso, F. Cardellach, J. Casademont, O. Miro, *Eur. Respir. J.* **2004**, *23*, 214-218.

25 M. Brand, *Exp. Gerontol.* **2000**, *35*, 811-820.

26 R. Arechederra, S. D. Minteer, *Electrochim. Acta* **2008**, *53*, 6698-6703.

27 C. Song, M. E. Scharf, *Pest Manag. Sci.* **2009**, *65*, 697-703.

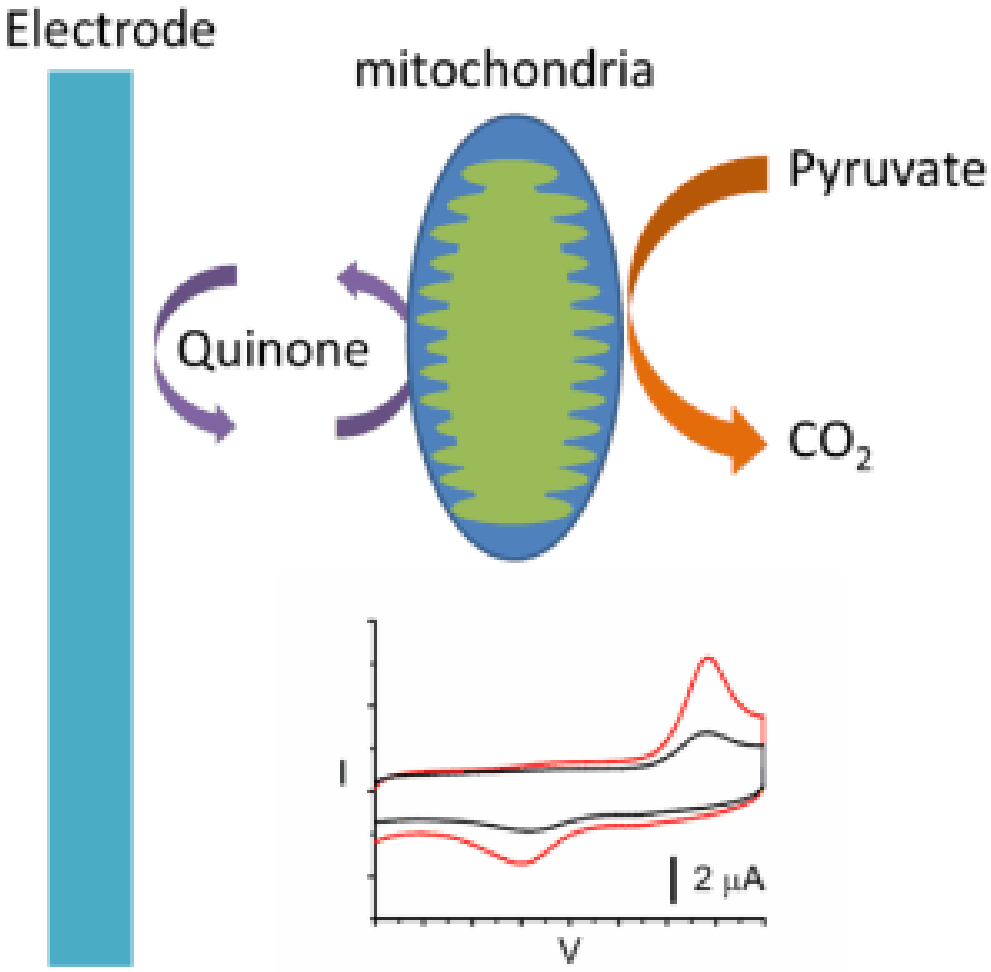

Figure 3.1: Schematic demonstration of the bioelectrocatalysis at a mitochondria modified electrode and cyclic voltammetry of mitochondria modified electrode tested in pyruvate solution (black line) and pyruvate solution containing 100 nM malathion (red line).

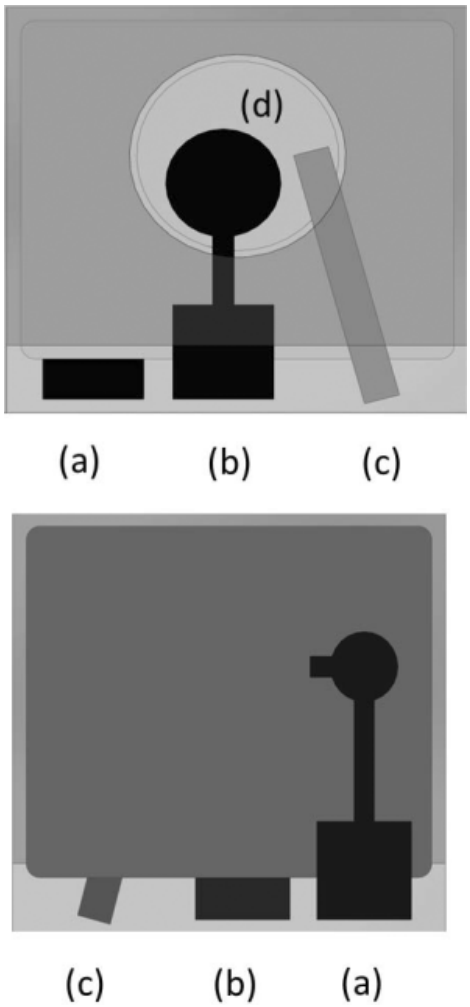

Figure 3.2: Schematic of a mitochondria three-electrode paper-based biosensor front view (above) and back view (below), showing (a) working electrode, (b) counter electrode, (c) Ag/AgCl reference electrode and (d) filter paper (Whatman) based, wax screen-printed sample pool.

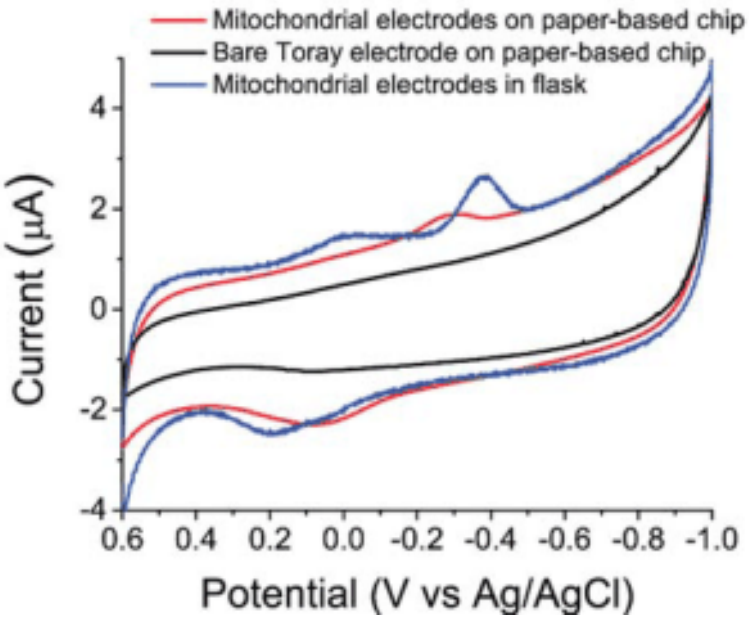

Figure 3.3: Representative cyclic voltammograms of mitochondria modified Toray paper electrodes in a standard three electrode system in solution (blue line) at 50 mV/s and representative cyclic voltammogram of bare (black line) or mitochondria modified (red line) electrodes in a paper-based device at 50 mV/s. Tests were performed in 100 mM phosphate-nitrate buffer containing 100 mM pyruvate, the tests were performed after nitrogen purging.

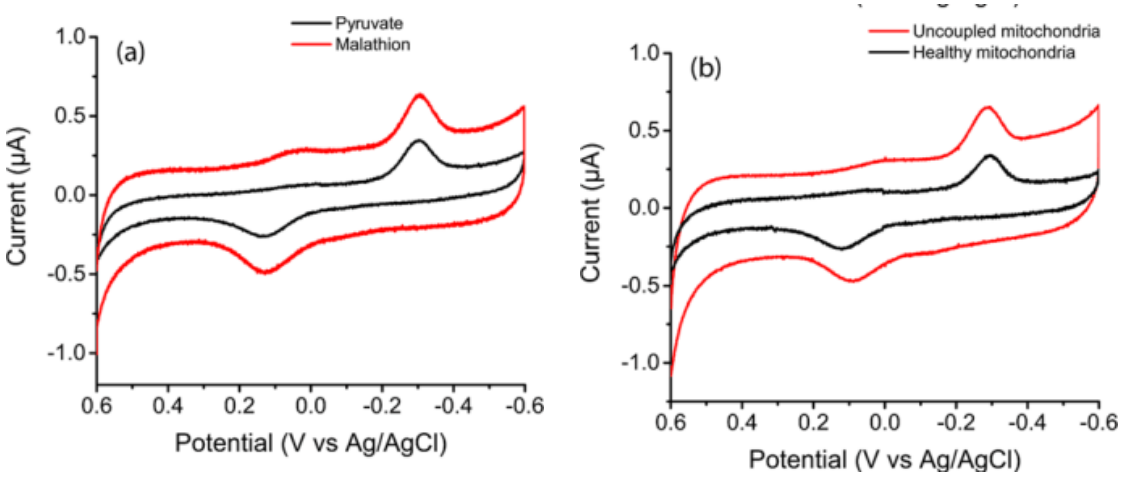

Figure 3.4: (a) Cyclic voltammogram of mitochondrial electrodes in 100 mM pyruvate solution (black) and 100 mM pyruvate solution containing 100 nM malathion (red) and (b) Cyclic voltammogram of healthy mitochondrial electrodes (black) and uncoupled mitochondrial electrode (red) in pyruvate solution. Scan rate: 10 mV/s, nitrogen purged, in a common lab setup.

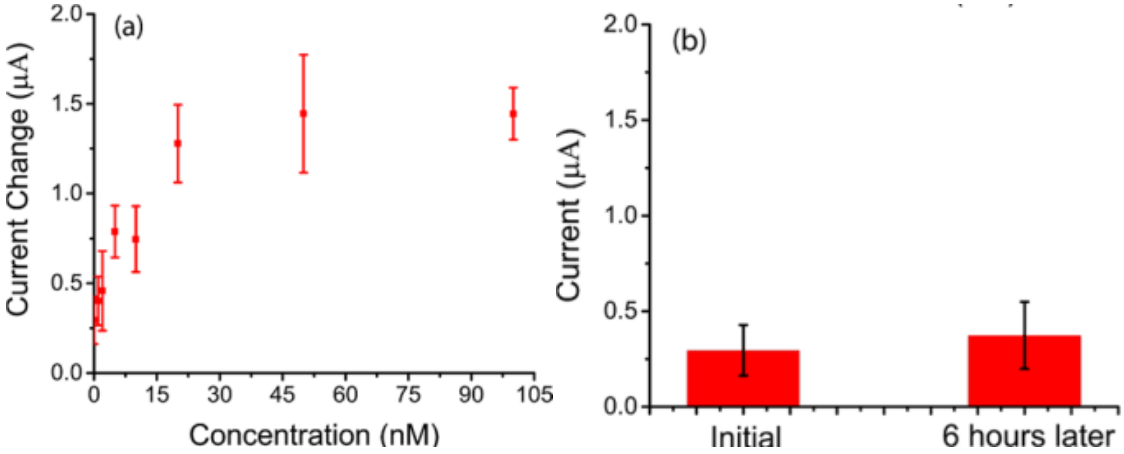

Figure 3.5: (a) Mitochondrial oxidative peak current change when exposed to different concentration of malathion, and (b) Mitochondrial oxidative peak current change over 6 hours.

CHAPTER 4

EFFECT OF RIBOFLAVIN METABOLITES ON MITOCHONDRIAL ELECTROCHEMISTRY

Mitochondrial deficiency is the cause of many diseases and the determination of changes in metabolic rates usually requires lysing of the mitochondria and isolating individual mitochondrial proteins. Alternatively, mitochondria can be immobilized on electrode surfaces to utilize electroanalytical evaluation of metabolic rates of intact mitochondria. However, the redox mechanisms are still poorly understood. In this chapter, the riboflavin cycle of mitochondria is studied electrochemically and its impact on mitochondrial voltammetry is discussed. The inhibition mechanism of mitochondria by three different inhibitors (rotenone, carboxin, and permethrin) is discussed and it is found that the inhibition behavior observed electrochemically is due to not only ubiquinone, which is the electrochemical communicating species of mitochondrial electrochemistry. It is also shown that riboflavin derivatives interact with ubiquinone leading to a change in the intensity of ubiquinone voltammetry peaks. This interaction is affected by altering the choice of solvent used during the electrode preparation process. Finally, it is concluded that the observed

voltammetry of mitochondrial inhibition is due to a change in riboflavin metabolism within the intact mitochondria immobilized on carbon electrodes.

4.1 Introduction

Mitochondria are the primary source of respiration and ATP synthesis for all eukaryotic cells. The mitochondrial electron transport chain (ETC), which is responsible for mitochondrial respiration, contains four proteins (three for fungal mitochondria) and ATP synthase as well as multiple electrochemically active species such as ubiquinone and cytochrome c. Mitochondria contain the proteins of the Krebs cycle[1-3] that are capable of metabolizing sugar metabolites, fatty acids[4] and amino acids[5] and have therefore been considered as attractive catalysts for bioelectrocatalysis applications such as biofuel cells, due to their high volumetric catalytic activity. The metabolism integrity and complexity also allows mitochondria to be responsive to many different toxins, such as inhibitors (rotenone, carboxin, etc.), uncouplers (dinitrophenol, dicumarol) and other toxins (cyanide, azide, CO), with different electrochemical responses toward different toxins.[6-7] Since mitochondrial ETC deficiency has been recognized as the reason for many diseases and disorders, like early age hypertonia, Kearns-Sayre syndrome, Alzheimer's and Leber's hereditary optic neuropathy,[8] an electrochemical biosensor incorporating mitochondria could possibly be an alternative biosensor technology to the current mitochondria deficient study that is based on mouse models.

The electrochemistry of mitochondria has been extensively studied. In

terms of practical application, mitochondrial fuel cells with advantageous fuel adaptation, power output and complete biofuel oxidation as well as mitochondrial biosensors with universality have been reported.[6-7,9-14]Mitochondria contain many different electrochemically active species, like flavin adenine dinucleotide (FAD),[4] riboflavin mononucleotide (FMN), ubiquinone,[15] and cytochrome c[4] which lead to discussions of mitochondrial electrochemical mechanisms, when mitochondria are immobilized at electrode surfaces. Li *et al*. suggest that mitochondrial electrochemistry is a function of FAD and cytochrome c separately. Using mitochondria from the liver of guinea pig in their publication, they declared that the electrochemistry of whole mitochondria has no difference compared to submitochondrial particles and the electrochemical species were determined by comparing mitochondrial redox potentials to the redox potential of FAD and cytochrome c individually.[4] Minteer *et al.* suggest that ubiquinone is the key species for mitochondria electrochemistry where research was based on the individual depletion of ubiquinone and cytochrome c to determine which species contributed to the resulting electrochemical response.[15-16] All of these electrochemical measurements have been done on carbon electrode surfaces, because there is good adhesion of the mitochondria to the carbon electrode surfaces compared to gold, ITO, etc.

Mitochondria are complex organelles that contain many electrochemically active species which may be involved in the electrochemical mechanism;[17] however, those redox active species were rarely included in previous discussions regarding mitochondrial electrochemistry. Also, mitochondrial inhibition has been

studied electrochemically in many different cases,[6-7] with limited discussion of the effect of those redox active species on the electrochemical inhibitory response. However, different from a typical enzymatic system where only a single enzyme or an enzyme cascade where all the components are known, mitochondria contain more than just the ETC, which is responsible for respiration, but also enzymes for the whole Krebs cycle as well as enzymes for vitamin metabolism and even enzymes for its own genetic system. Those biological systems consist of redox active substrates, products, cofactors, and enzymes that might also contribute toward mitochondrial electrochemistry. Among those electrochemical species, FMN/FAD are small, water-soluble redox active molecules that exist both in the mitochondrial matrix and the intermembrane space and are able to diffuse through the mitochondrial outer membrane, therefore making it possible for them to play a role in mitochondrial electrochemistry.

Therefore, as shown in Figure 4.1, we hypothesized that the electrochemistry of mitochondria on Toray paper electrodes are due to a contribution from both FMN/FAD and ubiquinone. In this paper, the interaction between FMN/FAD and ubiquinone is studied via dropcasting their mixture directly onto Toray paper electrodes and it is found that their interaction differs in aprotic and protic environments. One more portion of mitochondrial metabolism, the riboflavin/FAD cycle, is taken into consideration in order to explain the electrochemical behavior of mitochondria. An increase in the exportation of mitochondrial FMN/FAD is observed when mitochondria are inhibited. In summary, the cyclic voltammetry behavior of mitochondria during inhibition is

likely due to the exportation of FMN/FAD and the change of interaction between FMN/FAD and ubiquinone.

4.2 Experimental

4.2.1 Chemicals and materials

Fresh bovine heart was purchased from a local slaughter house (Dale T Smith&Sons, Draper, UT, USA) and soaked in MHSE buffer (70 mM sucrose, 210 mM mannitol, 5 mM HEPES, 1 mM EGTA, 0.5% (w/v) bovine serum albumin (BSA), pH 7.2) as well as kept on ice during the transportation process. Untreated Toray paper was purchased from Fuel Cell Earth (USA) and cut into 1 cm^2 squares and used without further treatment. All the other chemicals were purchased from Sigma-Aldrich (USA) and used as received.

4.2.2 Isolation of bovine heart mitochondria

Mitochondria were isolated from bovine heart based on a modified procedure from Rogers *et al.*[18] During the isolation, the bovine heart muscle was cut into 2 cm × 2 cm cubes and blended in a laboratory blender. Then the tissue was centrifuged at 26000x g for 10 min and the pellet was collected. Afterwards, the pellet was resuspended and centrifuged at 500x g twice and the supernatant was collected. Then the suspension was centrifuged at 10000x g twice, and the mitochondria were finally stored in 300 mM trehalose buffer (T buffer, 300 mM trehalose, 1 mM EDTA, 1 mM EGTA, 5 mM HEPES, 0.1% (w/v) BSA, 1% (w/v) polyethylene glycerol (PEG), pH 7.8).[19] Mitochondrial function was evaluated by

the Seahorse oxygen consumption assay to insure the isolated and purified mitochondria are intact and functional before use on an electrode.

4.2.3 Mitochondrial toxicity test

Mitochondrial suspension (200 mg mL^{-1}) was mixed individually with rotenone, permethrin or carboxin. The toxins were mixed with mitochondrial suspension individually at saturation (1 mg per 500 µL mitochondrial suspension) and the mixtures were vortexed for 30 min. The suspensions were cast on 1 cm^2 Toray paper electrodes immediately following the sonication process to prevent the precipitation of insolubilized toxin. The electrodes are then dried in a hood for approximately 30 min and then treated with TMOS vapor deposition, as described before,[15] in order to permanently immobilize the mitochondria on the electrode. To eliminate possible activity variation between different batches of isolated mitochondria, only the mitochondria from one batch of isolation were used in the test of one kind of toxins. Electrochemical evaluation was carried out in a standard 3-electrode electrochemical cell via cyclic voltammetry (CV) between −0.6 to 0.6 V (vs. Ag/AgCl (sat.)) for 2 cycles in nitrogen-purged 200 mM phosphate-nitrate buffer containing 0.5% (w/v) BSA. Pt mesh was used as the counter electrode. All negative currents correspond to oxidation currents.

4.2.4 Riboflavin derivatives electrochemical evaluation

FAD, FMN and ubiquinone were solubilized individually in water or ethanol at a concentration of 1 µM, mixed and co-cast on 0.25 cm^2 Toray paper

electrodes. Extra solvent was used during mixing to maintain a constant ratio of total solvent (water/ethanol). Electrochemical evaluation was carried out via cyclic voltammetry as described above.

4.2.5 Riboflavin assay

The export of riboflavin derivatives from mitochondria was monitored by UV-Vis on a Thermo-Fisher Nanodrop 2000. The mitochondrial suspensions (500 µL of 200 mg/mL) were first incubated with different inhibitors at room temperature for 30 min, lyophilized overnight, then resuspended in 50 µl T buffer and centrifuged at 10000x g for 10 min. The FAD/FMN content in the supernatant were measured by UV absorption at 390 nm.

4.2.6 Mitochondria lysate

Mitochondria were lysed by using surfactants and sonication, as per a standard literature procedure.[20] A Triton-X100 solution was mixed with the mitochondrial suspension at a ratio of 1:100 ml/mg protein, vortexed for 20 min and then sonicated with a Fisher-Scientific FB 505 sonicator for 2 min (4 cycles of sonication of 30 seconds and resting on ice for 1 min). The lysate were directly drop-cast on Toray paper electrode, prepared and tested following the same procedure as described above.

4.3 Results and discussion

4.3.1 Electrochemical characterization of mitochondria inhibition

The black lines in Figure 4.2 represent typical mitochondrial electrochemical behavior when immobilized on Toray carbon paper electrodes where a reduction peak at approximately −0.3 V (vs. Ag/AgCl) and an oxidation peak at approximately 0.15 V (vs. Ag/AgCl) are present that are due to ubiquinone.[15] Known Complex I inhibitors permethrin and rotenone[21-23] were tested on mitochondrial electrodes, while permethrin also interrupts mitochondrial sodium channels. None of those inhibitors are electrochemically active in the potential window of the experiment (Blue line, Figures 4.2A, 2B and 2C).[24] However, although both of those inhibitors affect ubiquinone reduction of complex I, their electrochemical behaviors are marginally different. As shown in Figure 4.2A, the inhibition of Complex I by permethrin resulted in an enhanced reduction wave and a diminished oxidation wave in cyclic voltammetry which is a function of the mitochondrial bioelectrocatalytic response toward the inhibition of ubiquinone reduction. Meanwhile with rotenone (as shown in Figure 4.2B), the mitochondrial oxidation and reduction wave were both diminished. It is shown in Figure 4.2 that although ubiquinone has been long reported as the key species in mitochondrial electrochemistry,[15] it may not be the only electrochemically active species involved in mitochondrial electrochemistry. To further study the inhibition behavior of mitochondria, a Complex II inhibitor (carboxin) was employed. Carboxin is a non-electrochemically active (Figure 4.2C) Complex II inhibitor[25-26] which also leads to a reduction of mitochondrial activity of quinone reduction. As

shown in Figure 4.2C, the loss of the ubiquinone reduction activity leads to a decrease of the peak height on both the reduction and oxidation peaks, similar to what was observed by rotenone-inhibited mitochondria (Figure 4.3). Therefore, it is hypothesized that ubiquinone is not the sole electrochemically active species involved in mitochondrial electrochemistry.

In previous studies, many different electrochemically active species in mitochondria have been tested (such as cytochrome c, ubiquinone, FAD and FMN). Based on the potential observed via mitochondrial cyclic voltammetry, it is unlikely that any other electrochemical species other than ubiquinone is the actual species involved in mitochondrial electrochemistry, because of the observed differences in redox potentials.[27-29] Meanwhile, this electrochemical behavior does not follow a typical prediction of electrocatalytic behavior following inhibition, indicating that although ubiquinone appears to be the predominant species of mitochondrial electrochemistry, there may be other electrochemically active species in mitochondria that are involved in mitochondrial electrochemistry.

Based on the fact that in the potential range of 0.6 to −0.6 V (vs. Ag/AgCl), none of the possible electrochemically active species (other than ubiquinone) present significant peaks in mitochondrial electrochemistry, indicating that mitochondrial inhibition electrochemistry is most likely due to a possible interaction between mitochondrial redox active species. One of the possible interactions between two mitochondrial electrochemically active species (NAD^+/NADH and ubiquinone) has been reported to be only capable of occurring

in a hydrophobic environment such as in a mitochondrial lipid membrane.[17] However, in this case, the interaction between NAD^+/NADH and ubiquinone during which ubiquinone acts as an electron mediator for the oxidation of NADH still follows a different pattern as observed during mitochondrial inhibition.

Another possible interaction, which is rarely reported, is between FMN/FAD and ubiquinone. FMN and FAD are cofactors of mitochondrial Complexes I and II as well as products/substrates of the mitochondrial riboflavin metabolism cycle. Moreover, FAD is also involved in the mitochondrial glycerophosphate shuttle. Considering all of these metabolic pathways combined, FMN and FAD appear in both mitochondrial matrices and the inter-membrane space. As reported, hydrophilic NAD^+/NADH could be chemically mediated via hydrophobic ubiquinone located in the lipid membrane;[17] therefore, it is hypothesized that FMN/FAD might interact with ubiquinone in a similar fashion.

To mimic the electrochemical conditions of the mitochondrial inhibition electrochemical analyses, Toray carbon paper was chosen as the electrode material and FMN/FAD, ubiquinone, and their mixtures were drop-cast on the electrode. Cyclic voltammetry of both FMN and FAD result in a single pair of redox peaks at approximately −0.4 V (vs. Ag/AgCl) (Figure 4.4) on Toray paper. As shown in Figure 4.5A, with the mixture of FMN and ubiquinone dissolved in ethanol and cast on a Toray paper electrode (while the ratio of FMN increases although the total amount of solvent remains the same), the ubiquinone oxidation peak current at approximately +0.1V (vs. Ag/AgCl) increases by 94 ± 20%, 156 ±

37% and 409 ± 69% as the ratio of FMN:ubiquinone increases from 0:1 to 1:1, 2:1 and 4:1. Additionally, FAD behaved in a similar fashion to FMN when mixed with ubiquinone (Figure 4.6). In this case, ubiquinone acts as an electron mediator for FMN. However, this redox pathway changes when water is present during the drop-casting process, as shown in Figure 4.5B. In this case, the oxidation peak current of ubiquinone decreases by 167 ± 4%, 272 ± 12% and 1489 ± 3% with the ratio of FMN:ubiquinone increase from 0:1 to 1:1, 2:1, and 4:1.

It is hypothesized that the observed mitochondrial electrochemistry could be a result of the interaction of FMN/FAD and ubiquinone. To demonstrate that such a system is being observed during mitochondrial electrochemistry (i.e. FAD/FMN enhance/decrease the electrochemical signal of ubiquinone with negligible electrochemical signal of itself appearing), a mixture of FAD, FMN and ubiquinone with a ratio of FAD:FMN:ubiquinone of 1:1:100 was drop-cast on Toray paper electrode for 14 hr while all the chemicals are dissolved in ethanol (Figure 4.7). It can be seen that FAD and FMN diffuse away from the electrode during evaluation; however, the enhancement of quinone redox peaks decreases by 17 ± 8% which is on a much smaller scale compared to the redox peaks associated with FMN/FAD which decreased by 95 ± 2%, indicating that this process is dominantly surface bound.[30]

To demonstrate that the hydrophobic environment created via the lipid membrane will result in a similar phenomenon, ubiquinone was dispersed in the lipid membrane and mixed with differing concentrations of FMN and cast on an

electrode. In this test, the ubiquinone oxidation peak increases at 115 ± 27%, 123 ± 14% and 810 ± 7% with the ratio of FMN:ubiquinone increase from 0:1 to 1:1, 2:1 and 4:1, with the existence of lipid membrane, even though FMN and ubiquinone were mixed in an aqueous solution.

To further demonstrate how this change in the local environment could affect the electrochemical response of mitochondrial electrochemical species, lysate of mitochondria was prepared. From Figure 4.5C, it can be seen that after lysing the mitochondria, both the mitochondrial oxidative and reductive peaks disappear. Since lysing will disrupt the lipid membrane in mitochondria, removing the hydrophobic environment maintained by it, therefore the electrochemistry behaves like the situation in Figure 4.5B, and finally leads to decrease or complete removal of mitochondrial redox peaks.

In mitochondria, riboflavin (vitamin B2) is metabolized to FMN and then FAD. During this process, riboflavin diffuses into the mitochondrial inter-membrane space and is then transported into the mitochondrial matrix via a riboflavin transporter, where it is metabolized to FMN and FAD.[31] In this process, four enzymes (riboflavin kinase, FAD synthetase, FAD pyrophosphatase, FMN phosphohydrolase) are involved as well as multiple carrier-based riboflavin transporting systems.[32] FMN and FAD are present in both the mitochondrial matrix and mitochondrial inner-membrane space. However, even though this interaction could be altered in vitro, whether their interaction in mitochondria occurs randomly or as a consequence of mitochondrial metabolism needs to be determined.

To demonstrate that the change of mitochondrial riboflavin metabolism could alter their electrochemical behavior, mitochondria were tested by feeding FMN/FAD as a substrate for riboflavin metabolism. Both FMN and FAD are capable of diffusing into the mitochondrial inter-membrane space; therefore, during testing they were directly mixed with the mitochondria and incubated at room temperature for 20 min. Since FAD pyrophosphatase is inhibited by EDTA in mitochondrial riboflavin metabolism,[33] mitochondria were transferred to trehalose buffer in the last stage of the mitochondria isolation process, which kept them coupled in the flash freeze-thaw cycle.[19] To prevent the inhibition of mitochondrial riboflavin metabolism, a portion of mitochondria were kept in their original buffer that contained only EGTA as a protease inhibitor. As shown in Figure 4.8, the addition of 10 mM FMN/FAD resulted in an increase of mitochondrial oxidation peak current when mitochondria were suspended only in MHSE buffer which contains no EDTA, while with the mitochondria suspended in trehalose buffer, no change is observed with the addition of FMN or FAD which indicates that the interaction of FMN/FAD and ubiquinone observed in vitro was not observed from the intake of external FMN or FAD; therefore, the interaction of FMN/FAD and ubiquinone is a consequence of mitochondrial riboflavin metabolism.

Since the mitochondria used in the inhibition test were suspended in trehalose buffer, the intake of riboflavin derivatives is inhibited (the synthesis of FMN/FAD is not likely to happen during this process). In active mitochondria, FMN and FAD are bound to riboflavoproteins as well as Complexes I and II.

Coupled mitochondria export FMN and FAD synthesized from riboflavin, FMN or FAD uptake, into cytosol.[32,34] It has also been demonstrated that mitochondria with ETC deficiency result in a shortage of riboflavin and derivatives thereof.[35] For the bovine heart mitochondria used in this research, we observed that the concentration of FMN/FAD in the supernatant of mitochondrial suspension increases from 38.1 ± 11.7 μM to 53.8 ± 9.4 μM (rotenone) and 66.6 ± 3.2 μM (carboxin) during the inhibition process. As a result of the increase of FMN and FAD export due to inhibition, an increase in the portion of the interaction between FMN/FAD and ubiquinone occurs in a protic environment, which causes the decrease of mitochondrial voltammetric peaks observed.

4.4 Conclusion

In this chapter, we report the voltammetric observation of mitochondrial inhibition via three different inhibitors (rotenone, permethrin and carboxin), which indicates that mitochondrial electrochemistry is not solely a function of ubiquinone mediation. Instead, it is shown that the intensity change of mitochondrial voltammetric peaks could reflect a change of mitochondrial metabolism related to its riboflavin cycle. Such a change of mitochondrial voltammetry during inhibition is a result of a change in the interaction of FMN/FAD and ubiquinone, which changes its mechanism in different chemical microenvironments. The understanding of such a mechanism shows that electrochemical methods can be used for assessment of mitochondrial deficiency, thus offering an alternative method which uses intact mitochondria,

therefore, avoiding the protein isolation process. Due to the additional mechanistic information, this method provides more information than just deficiency of the mitochondrial ETC. Also the surface interaction between ubiquinone and riboflavin derivatives provide a new path for enhancing the power output of mitochondrial biofuel cell or self-powered biosensors utilizing quinone or riboflavin derivatives as their electron mediators.

4.5 References

1 J. Holloszy, L. Oscai, I. Don, and P. Mole, *Biochem. Biophys. Res. Commun.,* **40** (6), 1368-1373 (1970).

2 K. LaNoue, W. J. Nicklas, and J. R. Williamson, *J. Biol. Chem.,* **245** (1), 102-111 (1970).

3 D. Sokic-Lazic and S. D. Minteer, *Electrochem. Solid-State Lett.,* **12** (9), F26-F28 (2009).

4 J. Zhao, F. Meng, X. Zhu, K. Han, S. Liu, and G. Li, *Electroanalysis,* **20** (14), 1593-1598 (2008).

5 D. Bhatnagar, S. Xu, C. Fischer, R. L. Arechederra, and S. D. Minteer, *PCCP,* **13** (1), 86-92 (2011).

6 S. L. Maltzman and S. D. Minteer, *Analytical Methods,* **4** (5), 1202-1206 (2012).

7. T. Wang, R. C. Reid, and S. D. Minteer, *Electroanalysis,* (2015).

8. D. C. Wallace, *Science,* **283** (5407), 1482-1488 (1999).

9. R. Arechederra and S. D. Minteer, *Electrochim. Acta,* **53** (23), 6698-6703 (2008).

10. R. L. Arechederra, K. Boehm, and S. D. Minteer, *Electrochim. Acta,* **54** (28), 7268-7273 (2009).

11. M. Zhou and J. Wang, *Electroanalysis,* **24** (2), 197-209 (2012).

12. D. Sokic-Lazic, R. L. Arechederra, B. L. Treu, and S. D. Minteer, *Electroanalysis,* **22** (7-8), 757-764 (2010).

13. M. N. Germain, R. L. Arechederra, and S. D. Minteer, *J. Am. Chem. Soc.,* **130** (46), 15272-15273 (2008).

14. M. N. Arechederra, C. N. Fischer, D. J. Wetzel, and S. D. Minteer, *Electrochim. Acta,* **56** (2), 938-944 (2010).

15. F. Giroud, T. A. Nicolo, S. J. Koepke, and S. D. Minteer, *Electrochim. Acta,* **110** 112-119 (2013).

16. S. J. Koepke, J. J. Watkins, and S. D. Minteer, *J. Electrochem. Soc.,* **163** (5), H292-H298 (2016).

17. W. Ma, D.-W. Li, T. C. Sutherland, Y. Li, Y.-T. Long, and H.-Y. Chen, *J. Am. Chem. Soc.,* **133** (32), 12366-12369 (2011).

18. G. W. Rogers, M. D. Brand, S. Petrosyan, D. Ashok, A. A. Elorza, D. A. Ferrick, and A. N. Murphy, *PloS one,* **6** (7), e21746 (2011).

19. R. Yamaguchi, A. Andreyev, A. Murphy, G. Perkins, M. Ellisman, and D. Newmeyer, *Cell Death Differ.,* **14** (3), 616-624 (2007).

20. H. C. Chan, D. Hughes, R. R. French, A. L. Tutt, C. A. Walshe, J. L. Teeling, M. J. Glennie, and M. S. Cragg, *Cancer Res.,* **63** (17), 5480-5489 (2003).

21. N. Li, K. Ragheb, G. Lawler, J. Sturgis, B. Rajwa, J. A. Melendez, and J. P. Robinson, *J. Biol. Chem.,* **278** (10), 8516-8525 (2003).

22. I. M. Møller, *Annu. Rev. Plant biol.,* **52** (1), 561-591 (2001).

23. J. R. Bloomquist, *Radcliffe's IPM World Textbook. University of Minnesota, St. Paul, Minnesota,* (2009).

24. S.-Y. Zhang, Y. Ito, O. Yamanoshita, Y. Yanagiba, M. Kobayashi, K. Taya, C. Li, A. Okamura, M. Miyata, and J. Ueyama, *Endocrinology,* **148** (8), 3941-3949 (2007).

25. J. Ulrich and D. Mathre, *J. Bacteriol.,* **110** (2), 628-632 (1972).

26. D. Mathre, *Pestic. Biochem. Physiol.,* **1** (2), 216-224 (1971).

27. C. B. Jacobs, M. J. Peairs, and B. J. Venton, *Anal. Chim. Acta,* **662** (2), 105-127 (2010).

28. M. Kamal, H. Elzanowska, M. Gaur, D. Kim, and V. Birss, *J. electroanal. chem. interfacial electrochem.,* **318** (1), 349-367 (1991).

29. M. J. Eddowes and H. A. O. Hill, *J. Am. Chem. Soc.,* **101** (16), 4461-4464 (1979).

30. L. Gorton and G. Johansson, *J. Electroanal. Chem. Interfacial Electrochem.,* **113** (1), 151-158 (1980).

31. M. Barile, C. Brizio, D. Valenti, C. De Virgilio, and S. Passarella, *Eur. J. Biochem.,* **267** (15), 4888-4900 (2000).

32. V. Bafunno, T. A. Giancaspero, C. Brizio, D. Bufano, S. Passarella, E. Boles, and M. Barile, *J. Biol. Chem.,* **279** (1), 95-102 (2004).

33. M. Barile, C. Brizio, C. Virgilio, S. Delfine, E. Quagliariello, and S. Passarella, *Eur. J. Biochem.,* **249** (3), 777-785 (1997).

34. A. N. Spaan, L. IJlst, C. W. van Roermund, F. A. Wijburg, R. J. Wanders, and H. R. Waterham, *Mol. Gen. Metab,* **86** (4), 441-447 (2005).

35. S. S. Perumal, P. Shanthi, and P. Sachdanandam, *Br. J. Nutr.,* **93** (06), 901-909 (2005).

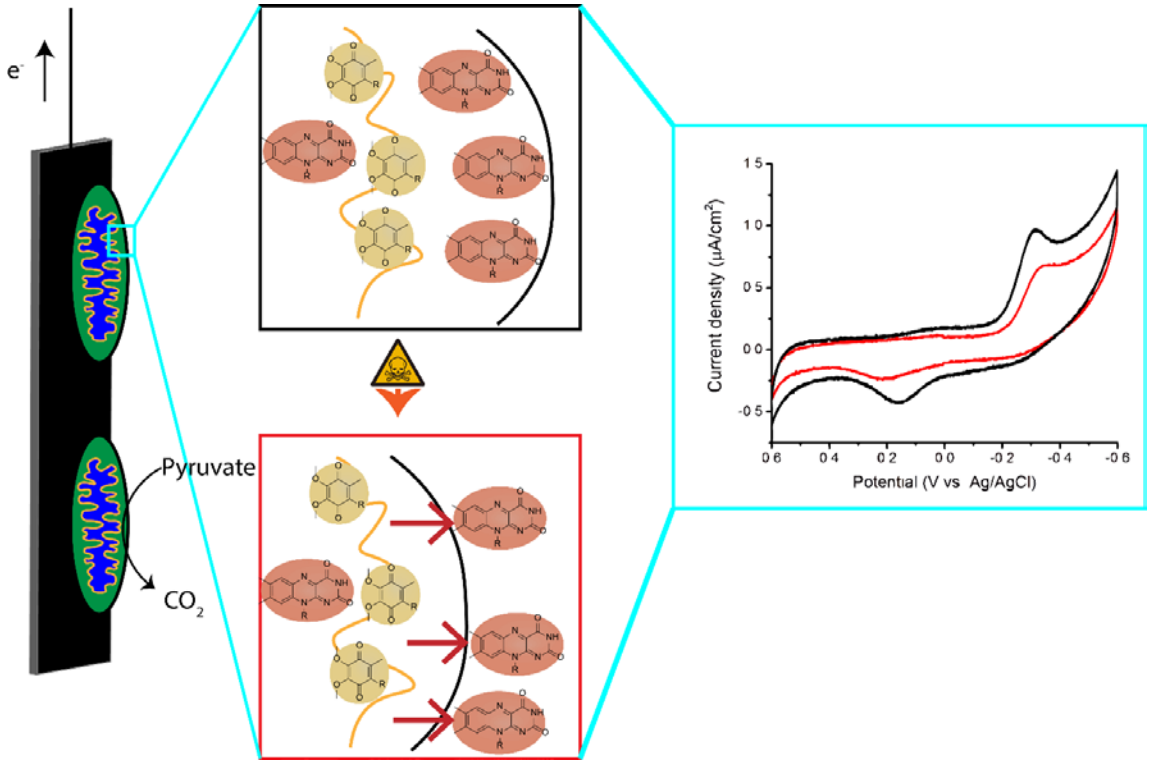

Figure 4.1: Mitochondrial riboflavin cycle in normal state (small figure, (A)) and during mitochondrial inhibition (small figure, (B)).

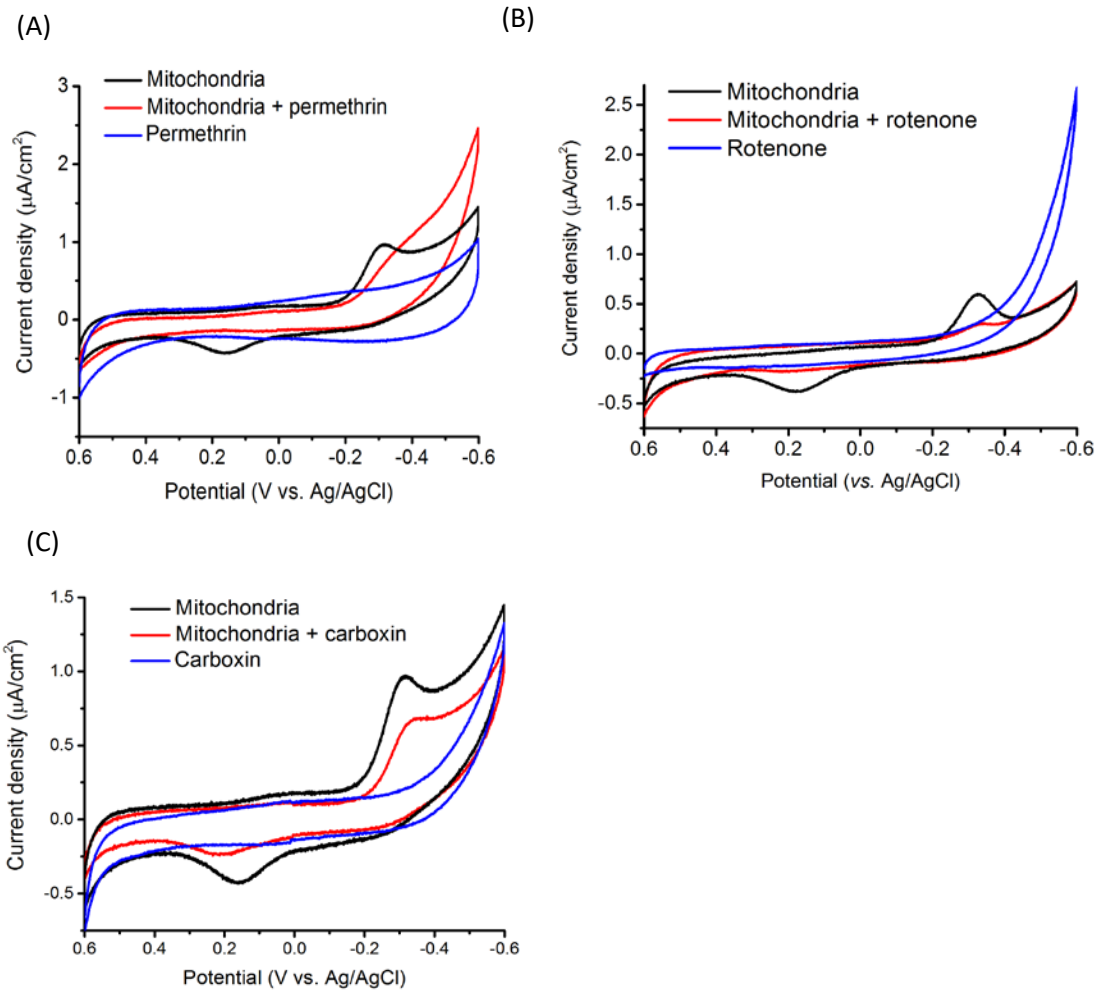

Figure 4.2: Representative cyclic voltammograms of mitochondria-modified Toray paper electrodes in 200 mM phosphate-nitrate buffer in the absence ((A), (B) and (C), black line) or presence of permethrin ((A), red line), rotenone ((B), red line) and carboxin ((C), red line), as well as permethrin ((A), blue line), rotenone ((B), blue line) and carboxin ((C), blue line) modified electrode. All experiments were performed at 10 mV/s with nitrogen purging to eliminate background O_2 reduction.

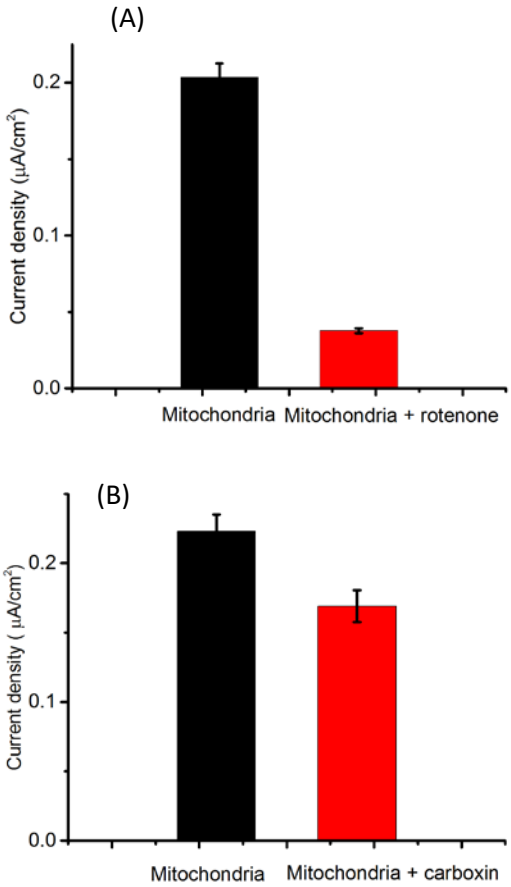

Figure 4.3: Background-subtracted oxidative peak current of mitochondria with (red bar) or without (black bar) the presence of rotenone (A) and carboxin (B). All tests were performed in 200 mM phosphate-nitrate buffer (pH 7.2, containing 0.5 % BSA) with nitrogen purging, the CVs were performed at 10 mV/s.

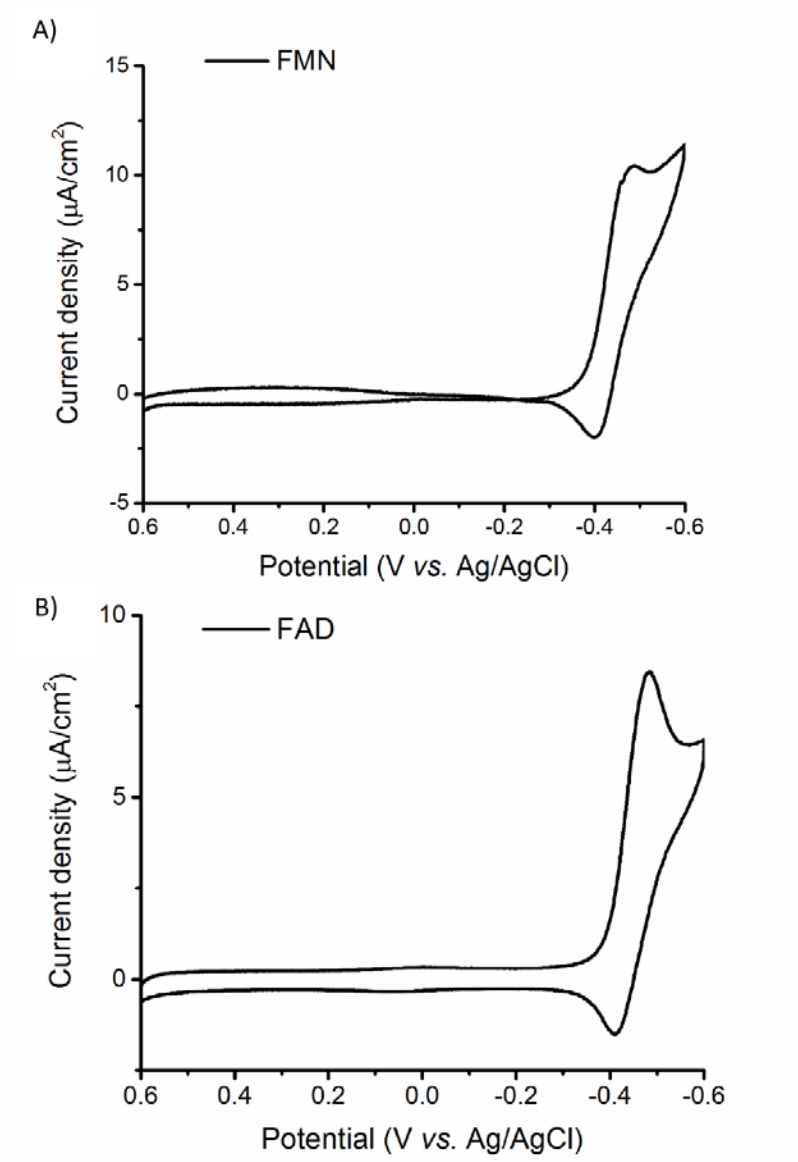

Figure 4.4: Representative cyclic voltammetry of FMN (A) and FAD (B) drop-cast on 1 cm^2 Toray paper electrode in 100 mM phosphate-nitrate buffer (pH 7.2, containing 0.5 % BSA). All experiments were performed at 10 mV/s.

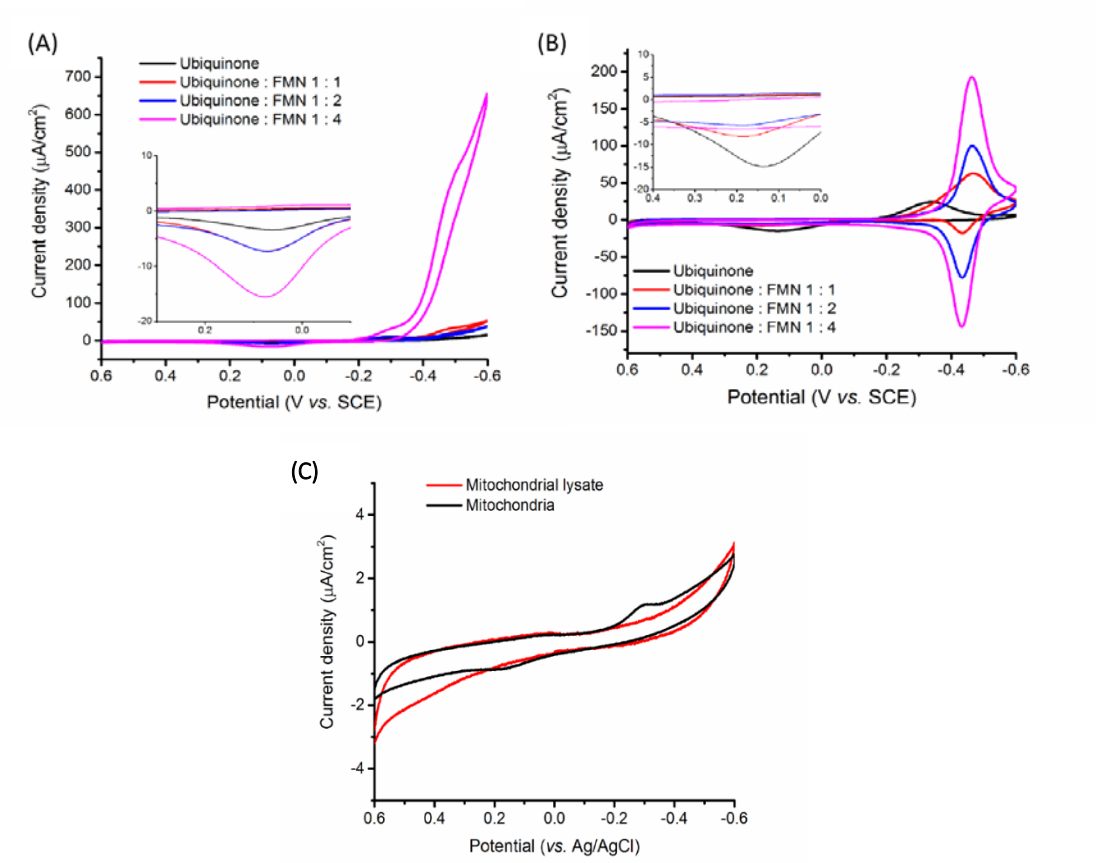

Figure 4.5: Representative cyclic voltammograms of FMN and ubiquinone mixture cast on Toray paper with different ratio of ubiquinone and FMN with (A) ubiquinone and FMN both dissolved in ethanol and (B) ubiquinone dissolved in ethanol and FMN dissolved in water. Figure (A) and (B) insets: enlargement of the ubiquinone oxidation peak in the corresponding figures. (C) Representative cyclic voltammetry of intact (black line) and lysed mitochondria (red line) in 200 mM phosphate-nitrate buffer with nitrogen purging. All experiments were performed at 10 mV/s.

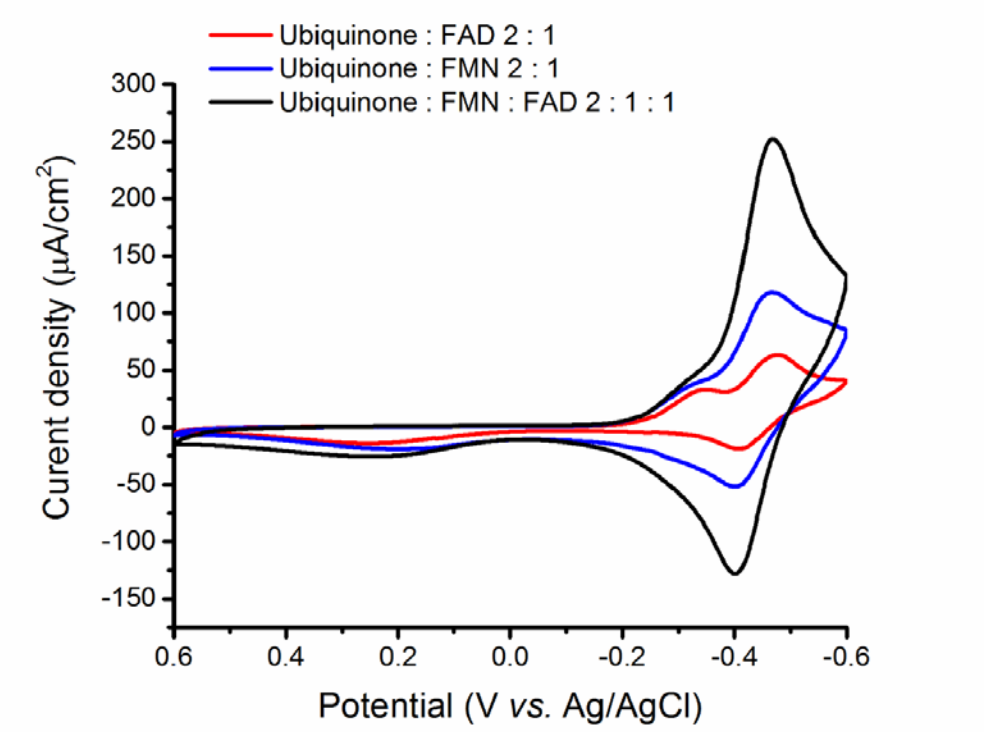

Figure 4.6: Representative cyclic voltammetry of ubiquinone-FMN/FAD mixture in 200 mM phosphate-nitrate buffer with the ratio of ubiquinone: FAD = 2: 1 (red line), ubiquinone: FMN =2: 1 (blue line) and ubiquinone: FMN: FAD= 2:1:1.

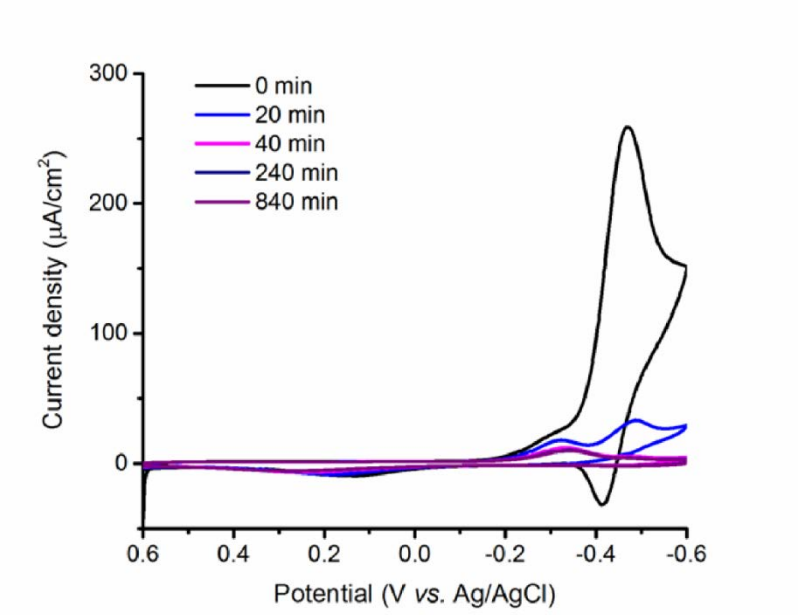

Figure 4.7: Representative cyclic voltammetry of FMN, FAD and ubiquinone mixture monitored over time, recorded at beginning (black line), 20 min (blue line), 40 min (pink line), 240 min (navy line) and 840 min (purple line). All experiments were performed in 200 mM phosphate-nitrate buffer.

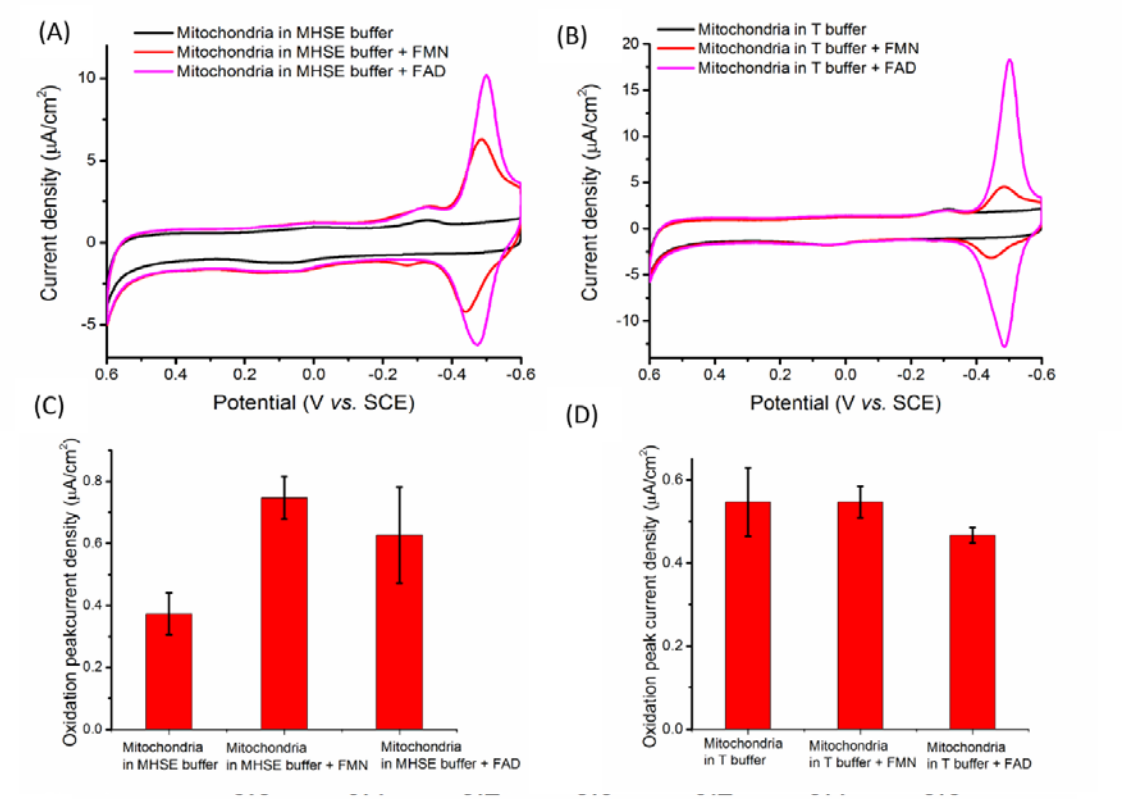

Figure 4.8: (A) and (B) cyclic voltammetry of mitochondria and their mixture with FMN and FAD with (A) mitochondria suspended in MHSE buffer and (B) mitochondria suspended in T buffer; (C) and (D) oxidation peak current of mitochondria and their mixture with FMN and FAD with (A) mitochondria suspended in MHSE buffer and (B) mitochondria suspended in T buffer. All tests were performed in 200 mM phosphate-nitrate buffer with nitrogen purging, at 10 mV/s.

CHAPTER 5

CONCLUSION AND FUTURE WORK

5.1 Conclusions

In this research, two biosensors were developed for groundwater monitoring, targeting two of the most commonly seen environmental pollutants - arsenic and pesticides (malathion). The emphasis on these projects was to observe the inhibition of the biotransducer, laccase or mitochondria, by environmental toxins and analyze the inhibition mechanisms.

In Chapter 2, the monitoring of arsenic (specifically, arsenite and arsenate) is performed via a laccase-modified biocathode. In this project, laccase is immobilized on anthracene-modified multilwalled carbon nanotubes. The purpose of anthracene-modified multiwalled carbon nanotubes is to orientate the T1 copper center of laccase towards the surface of the electrode due to the structural similarity of anthracene to the natural phenolic substrates of laccase. With the T1 copper site exposed and orientated towards the electrode, direct electron transfer was achieved for oxygen reduction catalyzed by laccase. The catalytic current of oxygen reduction catalyzed by laccase was observed to be decreased by the presence of arsenite and arsenate due to their inhibition effect on laccase. It was discovered that the catalytic current is regenerated after the removal of inhibitors

from the system (usually achieved by moving the laccase-modified electrode into a clean buffer solution); therefore, the inhibition of laccase by arsenite and arsenate was determined to be reversible.

The inhibition mechanism of laccase by arsenite and arsenate was further determined by Michealis-Menten nonlinear regression and Lineweaver-Burk double-reciprocal plots. The laccase activity assay was performed by UV-Vis under the wavelength of 420 nm using ABTS as substrate. It was determined that the inhibition of laccase by arsenite and arsenate falls under the mixed inhibition category. The sensitivity of laccase modified electrodes (with the presence of anthracene-modified multiwalled carbon nanotubes) was determined with amperometry at the potential of 0.2 V (vs. SCE) and was 46.9 ± 7.0 μA/mM and 10.6 ± 1.2 μA/mM for arsenite and arsenate, respectively. The corresponding linear dynamic ranges of laccase modified electrodes were approximately 0.5 – 5 mM for arsenite (R^2 = 0.9923) and 0.5 - 8 mM for arsenate (R^2 = 0.9894).

For a preliminary study of a field deployable biosensor, a self-powered biosensor was fabricated with a FAD-GDH anode and laccase cathode. It was found that the catalytic current of the FAD-GDH bioanode (utilizing ferrocene-LPEI as mediator) was not affected by the presence of arsenite or arsenate. Therefore, for the glucose/O_2 fuel cell-based self-powered biosensor, the power output of this fuel cell is solely affected by the cathode. With 100 mM glucose, the maximum power output reaches 57.2 ± 1.9 μW cm^{-2}. The glucose/O_2 fuel cell is operated at 10% of its maximum current and the potential of the fuel cell is reduced by the presence of arsenite and arsenate. Finally, the detection limit of this glucose/O_2

fuel cell was found to be 13 µM and 132 µM for arsenite and arsenate, respectively, and the sensitivities were 0.91 ± 0.07 mV/mM and 0.98 ± 0.02 mV/mM for arsenite and arsenate, respectively. The device showed a linear range of 1-20 mM for arsenite and 1-8 mM for arsenate, making it capable of detecting acute arsenic poisoning.

In Chapter 3, the isolation and characterization of mitochondria from bovine heart was discussed. Coupled mitochondria were isolated from bovine hearts obtained from a local slaughter house. Mitochondria were isolated by gradient centrifugation and the metabolism of mitochondria was studied by the seahorse oxygen consumption system. Coupled mitochondria were isolated from bovine heart and were tested against different environmental toxins. Mitochondria were transferred onto a paper-based platform. The paper-based platform was assembled from a filter-paper-based sample pool, Toray paper working electrode, Ag/AgCl reference electrode, and Pt-modified Toray paper counter electrode. The filter-paper based sample pool was fabricated via a wax screen-printing process. While the working and counter electrodes were fabricated by laser-cutting, the counter electrodes were further modified with platinum via electrodeposition. The Ag/AgCl reference electrodes were fabricated by oxidizing cured silver epoxy with $FeCl_3$ and coating it with agar as a salt bridge. Transfer of mitochondria from a normal laboratory set-up to the microfluidic chip was performed successfully, with only slight increases in capacitance and resistance.

The electrochemical behavior of isolated mitochondria was studied via cyclic voltammetry. As previously studied, the electrochemistry of mitochondria is

contributed to by ubiquinone inside the mitochondrial electron transport chain. However, coupled mitochondria showed two combined toxicity effects, inhibition and uncoupling. Mitochondrial uncoupling happens during mitochondrial apoptosis or when mitochondria are isolated from the original cellular environment. Mitochondrial uncoupling increases mitochondrial inner membrane permeability and allows more electrochemically active species to pass the mitochondrial membrane, resulting in an observed increase of capacitance and redox peak current. However, inhibition of the mitochondrial electron transport chain usually induces a decrease of mitochondrial electrochemical response, i.e. redox peak current. After comparing the mitochondrial response with inhibitors and uncouplers, a conclusion was drawn that the toxicity of malathion to mitochondria is due to uncoupling. Another study was performed to test the stability of isolated mitochondria using the mitochondrial redox current as the indication of mitochondrial uncoupling. It was found that 6 hours later, the mitochondrial current has no significant difference from the initial current, demonstrating that this mitochondria-based biosensor is stable enough to neglect the self-uncoupling of mitochondria. The performance of the biosensor was further characterized and was determined as an on-and-off sensor with a detection limit of 20 nM, capable for field-deployable tasks.

In Chapter 4, the electrochemical mechanism of mitochondria on Toray carbon paper electrodes was further studied. A few different mitochondrial inhibitors, like permethrin, rotenone, carboxin, and antimycin, were studied at a mitochondrial electrode. In previous studies, a significant response from

mitochondria to these toxins was difficult to obtain due to the low solubility of the toxin. Therefore, a new technique was used to observe the toxicity of these inhibitors with mitochondria. The inhibitors were incubated with mitochondria individually and co-cast with mitochondria on the electrode. A satisfactory result of mitochondrial inhibition induced by these inhibitors was observed and the result is contrary to the previous hypothesis.

In previous studies, ubiquinone was believed to be the sole electrochemically active species in mitochondrial electrochemistry; therefore, a typical electrocatalytic response was expected for inhibited mitochondria. However, such behavior was only observed for permethrin, while for rotenone, carboxin, and antimycin, the response manifested as a decrease or elimination of the mitochondrial electrochemistry response, indicating that ubiquinone might not be the sole electrochemically active species in mitochondria.

In this case, riboflavin derivatives were picked as a possible candidate the mechanism of mitochondrial electrochemistry. However, the redox potential of riboflavin was different from the potential observed for mitochondrial electrochemistry. In a further study of combined FMN and ubiquinone, it was found that riboflavin derivatives and ubiquinone had a synergistic effect when they are co-cast on Toray carbon paper electrode with ethanol as solvent. The electrochemical signal of ubiquinone was significantly enhanced when riboflavin derivatives were present (FMN, FAD). However, this effect could be easily altered by changing the solvent used during the drop-cast process. When water was present, the synergistic effect was altered to the other direction, i.e. the

electrochemical signal of riboflavin derivatives was enhanced. Such phenomena suggests that riboflavin derivatives act as the “switch” for the electrochemistry of ubiquinone inside mitochondria.

FMN and FAD are the cofactors of the mitochondrial electron transport chain enzymes (FMN is the cofactor of complex I, FAD is the cofactor of complex II). Mitochondria possess a whole system of riboflavin derivatives. To prove that the level of riboflavin in mitochondria is affected by mitochondrial inhibition, a photometric assay was performed by UV-Vis and it was observed that the concentration of riboflavin in the supernatant of the mitochondria suspension increased by almost 100% when mitochondria were exposed to inhibitors. It appears that mitochondria were releasing FMN/FAD into the supernatant, thereby altering the mitochondrial electrochemical response.

To further prove that mitochondrial lipid membranes offer a hydrophobic environment and make the synergy between the riboflavin derivatives and ubiquinone shift in the direction of enhancing the electrochemical response of ubiquinone, ubiquinone was suspended in lipid membrane and co-cast with FMN. It was shown that despite the existence of water in the mixture, with the presence of lipid membrane, the synergy of ubiquinone-FMN/FAD is still in favor of enhancing the electrochemical response of ubiquinone.

Attempts at altering the mitochondrial metabolism were performed and EDTA was used as an inhibitor for riboflavin transport in mitochondria to further prove that FMN/FAD could be an indication of mitochondrial metabolism change. By controlling the presence of EDTA in the buffer of mitochondrial suspension,

mitochondrial electrochemistry was altered by the addition of riboflavin derivatives. When EDTA was present, the addition of FMN/FAD had no effect on mitochondrial electrochemistry; however, when EDTA was removed, the addition of FMN/FAD increased the mitochondrial electrochemistry signal, showing that the changing of riboflavin metabolism has significant effect on mitochondrial electrochemistry. This finding improved the theory of using electrochemistry as a method for mitochondrial deficiency analysis.

5.2 Future work

5.2.1 Future improvements on laccase-based biosensor

In previous studies, the highest current of laccase is obtained by using anthracene-modified carbon nanotube[1]; however, in this case, the modification of multiwalled carbon nanotube, either through pyrene π-π stacking or covalent binding, limits the contact of laccase and electrode. For an electrochemical biosensor, increase of the current response is directly linked to the possible increase of signal-noise ratio; therefore, further improvements to the current output of laccase biocathode would improve the performance of the biosensor.

In previous studies in the Minteer group, redox polymer has been shown to provide significantly improved current over surface-modified carbon nanotubes. It has shown before that naphthoquinone can act in a similar role to anthracene to dock laccase towards the electrode.[2] Although in the previous reported work, naphthoquinone was immobilized through pyrene π-π stacking on multiwalled carbon nanotubes, a possible way to improve the oxygen reducing current of

laccase would be to immobilize laccase with naphthoquinone-modified redox polymers, such as naphthoquinone-LPEI.[3] However, based on previous results, anthracene-modified multiwalled carbon nanotubes still possess higher oxygen reducing current than naphthoquinone-modified carbon nanotubes. Therefore, investigations should also be done using an anthracene-based polymer for laccase immobilization for an even better oxygen-reducing current.

Another way to improve the current output of laccase biocathodes is to increase the oxygen concentration. For groundwater monitoring purposes, the laccase biocathode is operated in an aqueous environment where the concentration of oxygen in water is inherently limited by the solubility of oxygen in water. A recently published article indicates that incorporating lipids in an oxygen reducing system increased the oxygen reducing current of bilirubin oxidase, another oxygen reducing enzyme, by 2 fold.[4] Therefore, it is possible that this would be a potential method of increasing the oxygen-reducing current of laccase in an aqueous solution.

5.2.2 Future work on mitochondria-based biosensor

A current issue that the mitochondrial biosensor is facing is the lack of specificity. Ideally, a mitochondrial biosensor would be able to distinguish different environmental toxins since mitochondria carries five different enzymes in its electron transport chain and they perform different roles in terms of ubiquinone redox chemistry. However, the newest findings of mitochondria electrochemistry are that mitochondrial electrochemistry is a combined effect of FMN/FAD and

ubiquinone, and that mitochondrial inhibition induces FMN/FAD loss in mitochondria which reduces ubiquinone electrochemical signal. This leads to a lack of specificity in the mitochondrial biosensor, especially between the inhibition of complexes I, II, and III in mitochondria as they would all have similar response: reducing of electrochemical signal.

One way to increase the specificity of mitochondrial biosensors is to discover the electrochemical response from other electrochemically active species in mitochondria. Other than ubiquinone and FMN/FAD, the most probable electroactive species in mitochondria is cytochrome c. However, the molecular size of cytochrome c does not allow it to diffuse out of the mitochondrial intermembrane space. To make it possible to observe mitochondrial cytochrome c electrochemistry, a structural modification on mitochondria needs to be performed.

Since cytochrome c is a membrane bound protein that binds to the inner membrane of mitochondria and is confined in the mitochondrial intermembrane space, an easy strategy would be to remove the mitochondrial outer membrane. Such sub-mitochondria particles are called mitoplasts and their successfully preparation has been reported.[5-7] Preparation of mitoplasts mostly involves the use of surfactants to remove the outer membrane from mitochondria. In this case, quality control experiments will be vital for ensuring the intactness of mitoplasts. The seahorse oxygen consumption assay could be used to determine the functional integrity of mitoplasts with cytochrome c as one of the substrates. For the electrochemical characterization of mitoplasts, cytochrome c needs to be co-immobilized with mitoplasts to ensure the function of the mitochondrial electron

transport chain such that specific detection of mitochondrial complexes III and IV could be achieved.

It is notable that significant protein leaching was observed with the current TMOS immobilization technique, so it can be predicted that with cytochrome c and mitoplasts, the same issue may make the analysis of mitochondrial complexes III and IV inhibition problematic. To solve the protein leaching problem, a new immobilization method for mitochondria is needed. Cellulose is a biocompatible material that has been used for enzyme immobilization previously and is known to retain enzyme activity.[8-10] Therefore, it is an ideal candidate for co-immobilizing mitoplasts and cytochrome c.

The co-immobilization of cytochrome c and mitoplasts with cellulose can be performed in a layer-by-layer approach. Leaching of protein will need to be monitored with BCA protein assay. The lifespan of the mitoplast biosensor will be determined. A continuous test with seahorse oxygen consumption assay will be performed with cellulose immobilized cytochrome c and mitoplast. Finally, the biosensor will be tested against different mitochondrial inhibitors. It is expected that mitochondrial complexes III and IV inhibition could be observed via cytochrome c electrochemistry, while inhibition of mitochondrial complexes I, II, and III could be monitored via ubiquinone electrochemistry, thereby providing more specificity for the mitochondria-based biosensors.

In summary, both laccase and mitochondria-based biosensors have demonstrated their effectiveness in groundwater monitoring. Although, because of the stability of biological material, it is difficult to put biosensors into immediate

application for environmental monitoring at the moment. They are strong candidates for large-scale applications due to their advantageous size and instrumentation requirements in a field-deployable scenario.

5.3 References

1 Milton, R. D.; Giroud, F.; Thumser, A. E.; Minteer, S. D.; Slade, R. C. *PCCP* **2013**, *15*, 19371.

2 Giroud, F.; Milton, R. D.; Tan, B.-X.; Minteer, S. D. *ACS Catalysis* **2015**, *5*, 1240.

3 Milton, R. D.; Hickey, D. P.; Abdellaoui, S.; Lim, K.; Wu, F.; Tan, B.; Minteer, S. D. *Chemical Science* **2015**, *6*, 4867.

4 Hickey, D. P.; Knoche, K. L.; Albertson, K.; Castro, C.; Milton, R. D.; Minteer, S. D. *Chem. Commun.* **2016**, *52*, 13299.

5 Kinnally, K. W.; Campo, M. L.; Tedeschi, H. *J. Bioenerg. Biomembr.* **1989**, *21*, 497.

6 Hackenbrock, C. R. *J. Cell Biol.* **1972**, *53*, 450.

7 Decker, G.; Greenawalt, J. *J. Ultrastruct. Res.* **1977**, *59*, 44.

8 Khoshnevisan, K.; Bordbar, A.-K.; Zare, D.; Davoodi, D.; Noruzi, M.; Barkhi, M.; Tabatabaei, M. *Chem. Eng. J.* **2011**, *171*, 669.

9 Ong, E.; Gilkes, N. R.; Miller, R. C.; Antony, R.; Warren, J.; Kilburn, D. G. *Enzyme Microb. Technol.* **1991**, *13*, 59.

10 Ong, E., University of British Columbia, 1992.